ACI STRUCTURAL JOURNAL TECHNICAL PAPER

Title no. 103-S56

Punching of Reinforced and Post-Tensioned Concrete Slab-Column Connections

by Thomas H.-K. Kang and John W. Wallace

Data collected from shaketable tests of two, approximately 1/3-scale, two-story flat plate frames using shear reinforcement, as well as data from previous tests, were evaluated to assess the interstory drift ratios when punching failures occur for reinforced concrete and post-tensioned slab-column connections with and without shear reinforcement. The drift ratios at punching failures for the two shaketable specimens were approximately equal to values reported for quasi-static tests of isolated specimens without shear reinforcement; but substantially less than reported for quasi-static tests of connections with shear reinforcement. The review of test results indicates that the bilinear relation for lateral drift versus gravity shear ratio to assess the need for shear reinforcement at slab-column connections approved for ACI 318-05, Section 21.11, is generally conservative for typical connections of all connection types. The data also were used to assess parameters required for a simple shear-strength degrading model for slab-column connections.

Keywords: columns; reinforcement; seismic; slabs.

INTRODUCTION

Slab-column frames are commonly used to resist gravity and lateral loads in regions of low-to-moderate seismicity and well-established design requirements exist to avoid punching failures at the slab-column connections.[1] To avoid punching shear failures at slab-column connections, the shear stress on the slab critical section due to direct shear (V_u/b_od) and eccentric shear ($\gamma_v M_{u,unb}c/J_c$) cannot exceed the nominal shear stress capacity of the critical section ($v_n = v_c + v_s$), where γ_v is the portion of the unbalanced moment $M_{u,unb}$ transferred by eccentric shear (for example, typically 40% for square, interior columns), v_c and v_s are the nominal shear stress capacity provided by the concrete and the shear reinforcement, respectively. If the calculated shear stress exceeds the nominal shear stress capacity, a punching failure is anticipated, and the design must be modified until the stress is acceptable (for example, thicker slab, larger column).

For slab-column frames subjected to lateral displacements due to earthquakes, punching failures are possible even if the shear stress on the slab critical section does not exceed the nominal shear stress (that is, no stress-induced failure). In this case, it is hypothesized that the shear stress capacity of the critical section degrades (for example, Pan and Moehle[2] and Hawkins and Mitchell[3]), and punching failure occurs when the shear capacity degrades to the point where it equals the demand (Fig. 1). In this paper, this is referred to as a drift-induced failure to differentiate it from a stress-induced failure discussed in the preceding paragraph.

Experimental studies of reinforced concrete flat plate slab-column connections (for example, Pan and Moehle,[2,4] Moehle,[5] and Robertson and Durrani[6]) have shown that the magnitude of the gravity shear stress on the slab critical section adjacent to the column significantly influences the drift level at which a punching failure occurs. Although slab-column frames are commonly used for nonparticipating systems[1] in zones of high seismicity, no guidance is provided in ACI 318-02,[7] Section 21.11, for design of these systems.

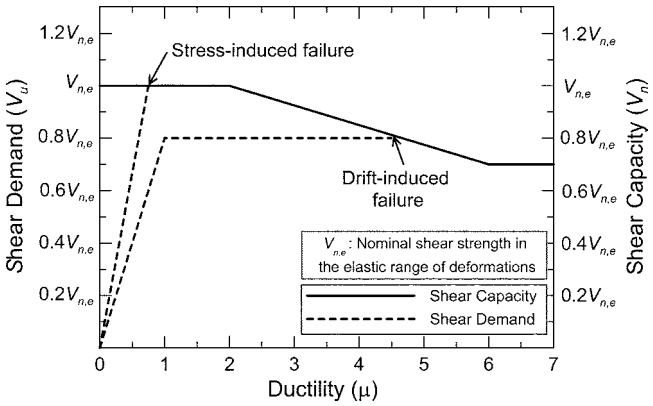

Fig. 1—Shear demand versus ductility relations and shear capacity versus ductility relations.

A code change was approved for ACI 318-05,[1] Section 21.11.5, to clarify the intent of the code with respect to checking the potential for punching failures of slab-column connections of nonparticipating frames. The new code provision assesses the need for shear reinforcement at slab-column connections based on the interstory lateral drift ratio and the gravity shear stress on the slab critical section. Alternatively, calculations can be made to show that the connection is capable of sustaining the drift associated with the design displacement without punching. The latter approach requires either a detailed analysis of the nonparticipating slab-column frame subjected to imposed lateral displacements or a limit analysis where maximum connection demands are determined. The use of a limit analysis appears attractive given the complexities of doing the detailed analysis, especially for cases where a fuse is used to limit the connection demands. This latter approach does not address the potential for shear strength degradation noted in Fig. 1, whereas use of the first approach, which is based on test results, incorporates potential strength degradation.

The relationship between gravity shear stress ratio, lateral drift ratio, and punching failure in ACI 318-05[1] as well as a best-fit line for test data derived from tests of isolated, reinforced concrete, slab-column connections without shear reinforcement (Table 1), are depicted in Fig. 2(a). Test

ACI Structural Journal, V. 103, No. 4, July-August 2006.
MS No. 04-378 received July 14, 2005, and reviewed under Institute publication policies. Copyright © 2006, American Concrete Institute. All rights reserved, including the making of copies unless permission is obtained from the copyright proprietors. Pertinent discussion including author's closure, if any, will be published in the May-June 2007 *ACI Structural Journal* if the discussion is received by January 1, 2007.

ACI member **Thomas H.-K. Kang** *is a Faculty Fellow at the University of California, Los Angeles (UCLA), Calif. He received his BS from Seoul National University, Korea; his MS from Michigan State University, East Lansing, Mich.; and his PhD from UCLA. He is a member of Joint ACI-ASCE Committee 352, Joints and Connections in Monolithic Concrete Structures. His research interests include performance-based earthquake engineering of reinforced and prestressed concrete structures, large-scale shaketable testing, and nonlinear analysis of structural systems.*

John W. Wallace, *FACI, is a Professor of Civil Engineering at UCLA. He is a member of ACI Committees 318-H, Structural Building Code; 369, Seismic Repair and Rehabilitation; 374, Performance-Based Seismic Design of Concrete Buildings; and Joint ACI-ASCE Committee 352, Joints and Connections in Monolithic Concrete Structures. His research interests include response and design of buildings and bridges to earthquake actions, laboratory and field testing of structural components and systems, and structural monitoring using sensor networks.*

results indicate that the lateral drift ratio at punching decreases as the gravity shear ratio increases, and results are conservative for the database of existing tests (only 4 of 76 tests fall below the ACI relation), which represent details used in typical construction of slab-column connections in areas of high and low-to-moderate seismic risk. For unusual geometries and quantities of reinforcement, a more detailed assessment of the potential for punching failure should be conducted. It is noted that relatively little data exist for gravity shear ratios greater than 0.6; however, for such large gravity shear ratios, the new ACI provision requires shear reinforcement unless the interstory drift is less than 0.005.

The use of shear reinforcement at slab-column connections has become a relatively common way to increase the punching shear capacity without increasing the effective depth of the slab (for example, providing drop panels). Stirrup placement can be cumbersome, therefore, alternatives such as stud-rails have been developed and shown to be effective.[8,9] Results plotted in Fig. 2(b) for connections with shear reinforcement indicate substantial scatter, with drift ratios at punching ranging from roughly 0.035 to 0.075 for a gravity stress ratio of approximately 0.5, and that relatively sparse data exist for gravity stress ratios greater than approximately 0.6. Robertson et al.[10] assessed the relationship between the lateral drift ratio at punching and gravity shear ratio for isolated connections with shear (stud-rail) reinforcement and recommended the relationship shown in Fig. 2(a) and (b). The relationship recommended by Robertson et al.[10] suggests that slab-column connections with shear stud-rails have roughly twice the drift capacity at punching for a given gravity shear stress ratio as connections without shear reinforcement (for $V_g/\phi V_c$ between approximately 0.2 and 0.6).

The existing database for post-tensioned connections is limited to three isolated slab-column interior connections tested by Qaisrani[11] (Fig. 2(b)). Results from these tests suggest that post-tensioned (PT) slab-column frames can sustain higher lateral drift ratios before punching than conventionally-reinforced slabs without shear reinforcement. The higher drift ratios may be in part due to the larger span-to-thickness ratios (l_1/h) used in PT slab-column construction relative to reinforced concrete (RC) construction (that is, ~25 for RC versus ~40 for PT; refer to Kang and Wallace[12]), as well as the increase of the shear strength of the slab-column critical section due to the in-plane compression forces f_{pc}

Table 1—Drift capacity at punching (reinforced concrete interior connections without shear reinforcement)

ID	h, mm	l_l, mm	$V_g/\phi V_c$	μ_θ	θ_y	$\theta_{u,model}$, (1)	$\overline{\theta}_{drift}$ (2)	$((1)-(2))^2 \times 10^4$	ID	h, mm	l_1, mm	$V_g/\phi V_c$	μ_θ	θ_y	$\theta_{u,model}$, (1)	$\overline{\theta}_{drift}$ (2)	$((1)-(2))^2 \times 10^4$
S1[2]	152	3660	0.33	3.00	0.010	0.030	0.038	0.56	SJB6[14]	150	1900	0.45	2.65	0.005	0.014	0.021	0.49
S2[2]	152	3660	0.45	2.65	0.010	0.027	0.020	0.43	SJB7[14]	150	1900	0.56	2.32	0.005	0.012	0.024	1.44
S3[2]	152	3660	0.45	2.65	0.010	0.027	0.020	0.42	8I[15]	114	2900	0.18	3.46	0.011	0.037	0.035	0.02
S4[2]	152	3660	0.40	2.79	0.010	0.028	0.026	0.04	I.I[15]	165	2900	0.08	3.76	0.007	0.028	0.050	5.07
S6[2]	152	3660	0.86	1.42	0.010	0.014	0.011	0.10	I[15]	80	2690	0.00	4.00	0.014	0.056	0.048	0.63
S7[2]	152	3660	0.81	1.58	0.010	0.016	0.010	0.34	2[15]	80	2690	0.00	4.00	0.014	0.056	0.040	2.44
S1[2]	76	1830	0.03	3.91	0.010	0.039	0.047	0.63	3[15]	80	2690	0.26	3.22	0.014	0.045	0.036	0.90
S2[2]	76	1830	0.04	3.90	0.010	0.039	0.028	1.20	4[15]	80	2690	0.30	3.10	0.014	0.043	0.024	3.77
S3[2]	76	1830	0.04	3.90	0.010	0.039	0.042	0.09	CD1[16]	150	1900	0.85	1.45	0.005	0.008	0.009	0.02
S4[2]	76	1830	0.08	3.77	0.010	0.038	0.045	0.54	CD2[16]	150	1900	0.65	2.05	0.005	0.011	0.012	0.01
S5[2]	76	1830	0.17	3.50	0.010	0.035	0.048	1.68	CD8[16]	150	1900	0.52	2.44	0.005	0.013	0.014	0.01
SM0.5[2]	152	1830	0.31	3.06	0.005	0.015	0.060	20.0	SC0[16]	89	2900	0.25	3.25	0.014	0.034	0.035	0.01
SM1.0[2]	152	1830	0.33	3.02	0.005	0.015	0.027	1.42	2C[6]	165	2900	0.18	3.46	0.007	0.025	0.035	0.09
SM1.5[2]	152	1830	0.30	3.10	0.005	0.016	0.027	1.32	6LL[6]	165	2900	0.53	2.43	0.007	0.018	0.009	0.85
INT[2]	61	1830	0.21	3.38	0.013	0.042	0.033	0.85	7L[6]	165	2900	0.37	2.89	0.007	0.021	0.015	0.37
AP1[2]	123	3660	0.37	2.89	0.012	0.036	0.016	3.95	1C[10]	150	3000	0.17	3.49	0.008	0.038	0.030	0.07
AP2[2]	123	3660	0.36	2.91	0.012	0.036	0.015	4.45	NDIC[17]	114	3048	0.25	3.25	0.011	0.036	0.050	1.93
AP3[2]	123	3660	0.18	3.45	0.012	0.043	0.037	0.33	ND4LL[17]	114	3048	0.37	2.89	0.011	0.032	0.040	0.62
AP4[2]	123	3660	0.19	3.45	0.012	0.043	0.035	0.59	ND5XL[17]	114	3048	0.48	2.56	0.011	0.028	0.020	0.71
IP2[2]	89	2740	0.18	3.45	0.013	0.044	0.050	0.31	ND6HR[17]	114	3048	0.30	3.10	0.011	0.034	0.050	2.56
IP3C[2]	89	2740	0.23	3.33	0.013	0.043	0.040	0.76	ND7LR[17]	114	3048	0.36	2.92	0.011	0.032	0.050	3.80
B7[2]	76	1830	0.04	3.88	0.010	0.039	0.038	0.69	H[18]	89	2290	0.28	3.16	0.011	0.037	0.040	0.09
C8[2]	76	1830	0.05	3.87	0.010	0.039	0.058	3.74	—	—	—	—	—	—	—	—	—

Notes: $\phi = 1$. μ_θ, θ_y, and $\theta_{u,model}$ = analytically determined values.

Table 2—Drift capacity at punching (reinforced concrete interior connections with shear reinforcement)

ID	$V_g/\phi V_c$	$\overline{\theta}_{drift}$	ID	$V_g/\phi V_c$	$\overline{\theta}_{drift}$
6CS[8]	0.24	0.040	2CS[10]	0.16	0.080
7CS[8]	0.24	0.037	3SL[10]	0.10	0.080
8CS[8]	0.27	0.050	4HS[10]	0.15	0.080
CD3[8]	0.91	0.035	SJB1[10]	0.48	0.055
CD4[8]	0.62	0.048	SJB2[10]	0.47	0.057
CD6[8]	0.64	0.054	SJB3[10]	0.48	0.050
CD7[8]	0.51	0.056	SJB4[10]	0.43	0.064
SS1[8]	0.49	0.035	SJB5[10]	0.47	0.076
SS3[8]	0.48	0.041	SJB8[10]	0.46	0.057
SS4[8]	0.47	0.055	SJB9[10]	0.49	0.071
SS5[8]	0.42	0.049	4S[6]	0.16	0.035

Note: $\phi = 1$.

generated by the PT (generally 1.03 to 1.38 MPa [150 to 200 psi]). The impact of the in-plane compression on the drift capacity at punching can be assessed using Fig. 2(a) with a modified nominal shear strength (that is, Eq. (11-36) of ACI 318-05[1]), whereas the influence of the span-to-thickness ratio is addressed later in this paper.

Available information for assessing the punching shear capacity of slab-column connections in intermediate moment frames[1] and nonparticipating frames[1] subjected to cyclic loads is rather limited for cases where shear reinforcement is used, particularly for post-tensioned floor systems. In addition, no test results have been reported for post-tensioned systems subjected to dynamic loads, and limited studies have been conducted to develop and verify shear-strength degrading models. Given that post-tensioned floor systems with shear reinforcement are commonly used for nonparticipating frames in regions of high seismicity, the objectives of the study reported herein were to conduct shaketable studies on two, approximately 1/3-scale slab-column frames and to use data from these tests, along with data from previous tests, to address these critical gaps. The two-story specimens consisted of a conventionally-reinforced (RC) frame and a PT frame with nominal bonded reinforcement.

RESEARCH SIGNIFICANCE

New code provisions in ACI 318-05[1] require that the potential for punching shear failures at slab-column connections of nonparticipating frames be evaluated. The new provisions are based primarily on tests of isolated, reinforced concrete slab-column connections subjected to quasi-static loading. Available test data for PT and shear reinforced connections, though limited in quantity, indicate that the drift capacity at punching is roughly twice that for RC connections. A detailed review of existing test data, as well as new data from shaketable tests on two slab-column frames, are used to assess the new provisions, as well as to determine best-fit parameters for a shear-strength degrading model for slab-column connections.

REVIEW OF PREVIOUS EXPERIMENTAL RESEARCH

The influence of the direct gravity shear stress on the lateral-load ductility of slab-column connections has long been recognized.[13] A review of the relationship between punching failure and lateral drift capacity as influenced by the gravity shear stress ratio for RC slab-column connections and frames, with and without post-tensioning reinforcement, is presented in the following subsections.

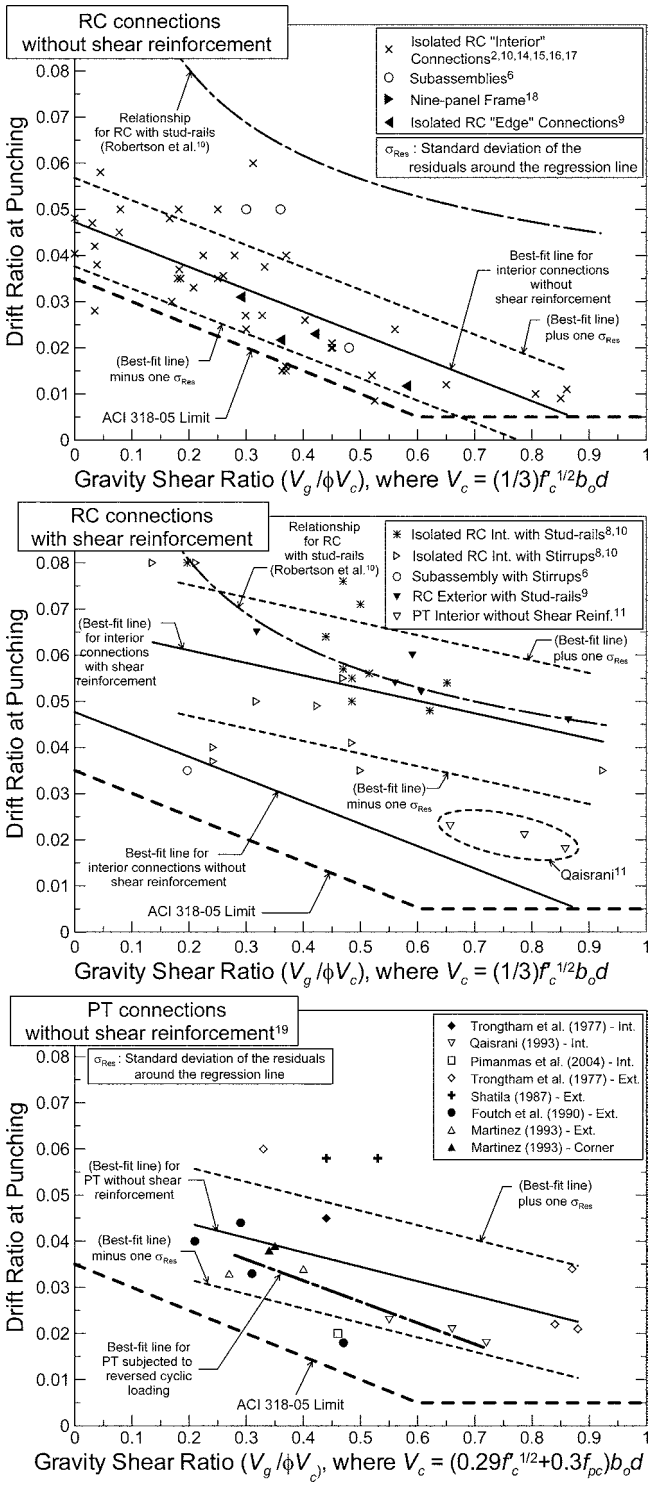

Fig. 2—Drift ratio at punching versus gravity shear ratio.

Reinforced concrete slab-column connections

Pan and Moehle[2,4] and Moehle[5] reviewed test results for 23 isolated, RC slab-column interior connections without shear reinforcement (Table 1) to study the influence of the direct gravity shear stress on lateral-load ductility. This data-

Table 3—Drift capacity at punching (post-tensioned connections without shear reinforcement)[19]

Authors (loads)	ID (type)	f'_c, MPa	f_{pc},* MPa	d,† mm	b_o, mm	$V_g/\phi V_c$	$\overline{\theta}_{drift}$	Authors (loads)	ID (type)	f'_c, MPa	f_{pc},* MPa	d,† mm	b_o, mm	$V_g/\phi V_c$	$\overline{\theta}_{drift}$
Trongtham and Hawkins[23] (1977, RP)	S1 (I)	26.9	1.12	104	1854	0.84	0.022	Shatila (1987, RP)	S1 (E)	35.8	3.73	119	991	0.53	0.058
	S2 (E)	29.0	1.91	112	1295	0.44	0.041		S5 (E)	41.3	3.93	119	1118	0.44	0.058
	S3 (I)	25.5	1.12	104	1854	0.87	0.034	Martinez (1993, RC)	E1 (E)	33.1	1.37	74	737	0.35	0.039
	S4 (I)	26.2	1.12	104	1854	0.88	0.021		E2 (E)	31.8	1.46	74	737	0.34	0.038
	S5 (I)	24.8	1.12	104	1854	0.33	0.060		C1 (C)	40.6	1.54	74	457	0.40	0.034
Foutch et al.[24] (1990, M)	S1 (E)	50.4	3.10	84	1092	0.21	0.040		C2 (C)	42.3	1.46	74	457	0.27	0.033
	S2 (E)	42.8	3.52	84	1092	0.31	0.033	Qaisrani[11] (1993, RC)	I1 (I)	28.1	1.66	71	1092	0.72	0.018
	S3 (E)	42.1	2.21	84	1092	0.29	0.044		I2 (I)	28.1	1.66	71	1092	0.66	0.021
	S4 (E)	48.3	2.21	84	1092	0.47	0.018		I3 (I)	27.7	1.66	71	1092	0.55	0.023
Pimanmas et al. (2004, RC)		40.4	1.66	71	1778	0.46	0.020								

Notes: $\phi = 1$; (I) = interior; (E) = exterior; (C) = corner; (M) = monotonic; (RP) = repeated; and (RC) = reversed cyclic.

*Average f_{pc} in two directions.

†Average distance from extreme compression fiber to centroid of post-tensioning tendons in two directions (interior) or distance from extreme compression fiber to centroid of post-tensioning tendons in direction parallel to slab edge (exterior).

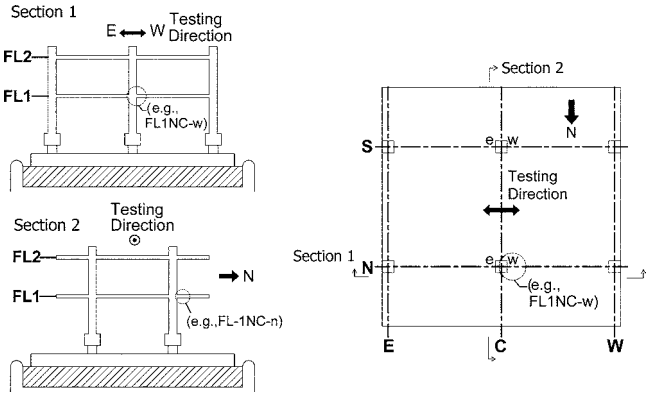

Fig. 3—Test specimen on shaketable.

base was extended by: 1) Dilger and Brown,[14] Luo and Durrani,[15] Hueste and Wight,[16] and Robertson et al.[10,17] to add results from 18 isolated, RC slab-column interior connections tested without shear reinforcement; 2) Robertson and Durrani[6] to add results for three interior connections based on tests on slab-column subassemblies consisting of one interior and two exterior connections; and 3) Hwang and Moehle[18] to add results for a nine-panel frame subjected to biaxial cyclic lateral drift.

Based on the review of the data plotted in Fig. 2(a), a clear trend of decreasing drift at punching for increasing gravity shear ratios ($V_g/\phi V_c$) is noted, when ϕ is 1.0 and using as-measured material properties. Trends in the data from the additional studies reported in Table 1 for isolated, RC connections are consistent with the previous observations.

Although limited data are available for reversed-cyclic tests of reinforced concrete exterior connections without shear reinforcement,[9] results plotted in Fig. 2(a) for four specimens indicate that the trend for interior connections also applies to exterior connections. Test results for isolated, reinforced concrete slab-column connections with shear reinforcement (Table 2; Fig. 2(b)) were assembled by Megally and Ghali,[8] and Robertson et al.[10] to study the influence of gravity shear ratio ($V_g/\phi V_c$) on punching failures. Trends noted in Fig. 2(b) indicate that isolated connections with shear reinforcement tested under quasi-static reversed cyclic loads achieved significantly larger drift ratios than the isolated connections tested without shear reinforcement. It is also noted that the drift capacity for specimens with stud-rails is approximately 35% higher than those without stirrups for gravity shear ratios between 0.15 and 0.50).

Post-tensioned slab-column connections

For post-tensioned slab-column connections, the database of available tests (Table 3; Fig. 2(c)) includes eight interior, nine exterior, and two corner connections without shear reinforcement. These studies include specimens without shear reinforcement subjected to monotonic (4), repeated (7), and reversed cyclic (8) lateral loading. The gravity shear force on some of the connections was increased at specific times during the test for 11 of the 19 test specimens, versus being held constant for the duration of the test; therefore, only the gravity shear stress ratio at punching is reported in Table 3. For PT connections, V_c is calculated using the provisions of ACI 318-05,[1] Section 11.12.2.2. An overview of each test program and a detailed assessment of drift capacities at punching for each test are provided by Kang.[19]

Shaketable studies of reinforced concrete and post-tensioned slab-column systems

Relatively few studies of the dynamic responses of flat plate systems have been conducted.[12,20,21] Of these studies, the specimens tested by Moehle and Diebold[20] and Hayes et al.[21] included perimeter beams; punching failures at individual interior connections were not assessed. The overall test configuration for the two, approximately 1/3-scale, two by two bay, two-story specimens tested by Kang and Wallace[12] is shown in Fig. 3. The slab span-to-thickness ratios (l_1/h) are 23.1 (RC) and 37.3 (PT), and the gravity shear ratios ($V_g/\phi V_c$) for a design strength of f'_c = 28 MPa (4 ksi) for the interior connections were 0.33 and 0.44 for the RC and PT slabs, respectively, where $\phi = 0.75$. Shear reinforcement, in the form of stud-rails, was used to increase the nominal shear strength of the slab-column connections. The specimens were subjected to several runs of uniaxial shaking using the CHY087W record[22] from the Sept. 21, 1999, M 7.6 Chi Chi earthquake in Taiwan, with the intensity of shaking increased for each subsequent run. Results presented in the following sections were obtained for damage-level excitation (Run 4; refer to Kang and

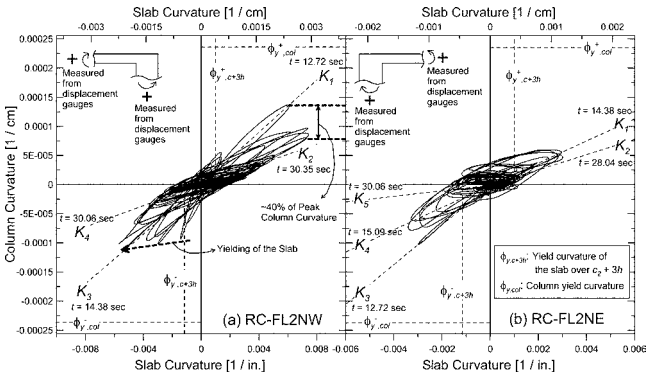

Fig. 4—Slab curvature versus column curvature (reinforced concrete exterior connections).

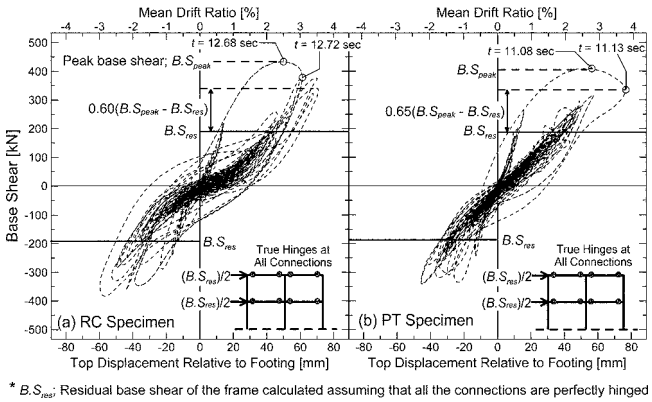

* $B.S_{res}$: Residual base shear of the frame calculated assuming that all the connections are perfectly hinged

Fig. 5—Base shear versus mean drift ratio.

Wallace[12]) for both the RC and PT specimens. More detailed information on the tests is provided by Kang and Wallace[12] and Kang.[19]

PUNCHING FAILURES—SHAKETABLE TESTS

Relationships for drift capacity at punching versus gravity shear ratio for individual connections of the specimens were assessed using a variety of approaches. For the individual connections, it was possible to assess punching by examining the relationship between slab and column curvatures,[19] where curvatures were calculated as the difference between either two reinforcing bar strain gauge readings or two average strain readings obtained using displacement gauge readings (divided by the sensor gauge length) on opposite sides of a column or a slab, divided by the distance between the gauges. Because yield of column longitudinal reinforcement did not occur other than at the base of the first story, a drop in the column curvature (or moment) for increasing slab curvatures indicates a drop in the unbalanced moment being transferred to the column (that is, punching). In some cases, however, insufficient quality data existed to reliably determine these relationships. In such cases, punching was assessed by examining the story shear versus interstory drift relations. For the RC specimen, both approaches were used (for most connections), whereas for the PT specimen, only the latter approach was used.

Findings for the RC and PT specimens are compared with results obtained from prior tests conducted under quasi-static monotonic and cyclic loading of isolated connections to investigate the importance of key parameters, such as the influence of post-tensioning, shear reinforcement (stud-rails), and load history (dynamic versus quasi-static).

Reinforced concrete specimen—exterior connections

Slab curvature versus column curvature relations for the exterior roof level connections of the RC specimen are presented in Fig. 4. For negative bending, Fig. 4(a) (RC-FL2NW, refer to Fig. 3 for notation) reveals that yield of slab flexural reinforcement occurs at close to the calculated yield curvature ϕ_y, and that the column curvature remains relatively constant at –0.001/cm for a large range of slab curvatures (–0.0004 to –0.0025/cm) without loss of moment transfer capacity. Degradation in moment transfer capacity appears to initiate at approximately t = 14.38 seconds, where the ratio of column to slab curvature is reduced from K_3 = 0.054 (t = 14.38 seconds) to K_4 = 0.023 (t = 30.06 seconds). For positive bending, results plotted in Fig. 4(a) indicate that a punching failure occurred for FL2NW connection of the RC specimen between t = 12.71 and 12.73 seconds, as the column curvature drops by 40%. The smaller value of K_2 (= +0.022 at t = 30.35 seconds) relative to K_1 (= +0.057, t = 12.72 seconds) is a result of a punching failure. The slab curvature versus column curvature plot for the other exterior roof level connection (Fig. 4(b); RC-FL2NE) displays similar features, with punching failure noted for negative bending. Reinforcement strains were measured using strain gauges affixed to the reinforcing bars to verify that slab reinforcement strains within $c_2 + 3h$ exceeded yield and column reinforcing bar did not yield, where c_2 is the column dimension perpendicular to the direction of the applied loads.[12,19]

Table 4—Interstory drift capacities at punching

	Time, seconds	$V_g/\phi V_c$	$\bar{\theta}_{drift}$
Reinforced concrete—mean drift	12.68	0.25	0.0250
	17.72	0.25	0.0307
Reinforced concrete—second-story drift	12.68	0.25	0.0256
	12.72	0.25	0.0335
Post-tensioned—mean drift	11.08	0.33	0.0278
	11.13	0.33	0.0377
Post-tensioned—second-story drift	11.08	0.33	0.0304
	11.13	0.33	0.0425

Note: ϕ = 1.

Reliable column curvature data were not obtained at exterior connections at the first floor level. However, because the unbalanced moment transferred at the first floor level connections is expected to be greater than the unbalanced moment transferred at the roof level (given that the same gravity load and reinforcement existed at both levels, and the higher rotational stiffness of the connection), punching failures were expected to occur at the first-floor level exterior connections. Based on the observed degradation of the base shear versus top displacement relations, punching at the first-story exterior connections was estimated to occur between t = 12.68 and 12.72 seconds (Fig. 5(a)).

The drift levels at punching for the connections of the test specimens were determined using two approaches as: 1) the average of the interstory drift ratios for the stories above and below a connection ($\bar{\theta}_{drift}$ in Table 4), and 2) the average of slab rotations on either side of the connection ($\bar{\theta}_{rot}$ in Table 5; Fig. 6). For the first approach, results are determined from the measured story displacements (for example, Fig. 5), whereas for the second approach, slab rotation θ_{rot} on either side of a connection was calculated as the sum of the slab

Table 5—Slab rotation capacity at punching (reinforced concrete specimen)

	Time, seconds	θ_y, rad	$\theta_{pl,low}$, rad	$\theta_{pl,avg}$, rad	$\theta_{pl,high}$, rad	$\theta_{rot,low}$, rad	$\theta_{rot,avg}$, rad	$\theta_{rot,high}$, rad	$\overline{\theta}_{rot}$*	$V_g/\phi V_c$
FL1NC-w	12.68	0.0159	–0.0122	–0.0153	–0.0183	–0.0281	–0.0311	–0.0342	0.0251 ~ 0.0279	0.25
	12.72	0.0159	–0.0155	–0.0194	–0.0233	–0.0314	–0.0352	–0.0391		
FL1NC-e	12.68	0.0176	0.0012	0.0015	0.0018	0.0188	0.0191	0.0194		
	12.72	0.0176	0.0024	0.0030	0.0036	0.0200	0.0206	0.0212		
FL2NC-w	12.68	0.0159	–0.0059	–0.0074	–0.0088	–0.0217	–0.0232	–0.0247	0.0270† ~ 0.0317†	0.25
	12.72	0.0159	–0.0087	–0.0109	–0.0131	–0.0246	–0.0268	–0.0289		
FL2NC-e	12.68	0.0176	0.0106	0.0132	0.0159	0.0282	0.0308	0.0335		
	12.72	0.0176	0.0153	0.0191	0.0229	0.0329	0.0367	0.0405		
FL1NE	12.68	0.0176	–0.0134	–0.0168	–0.0042	–0.0293	–0.0326	–0.0359	–0.0326	0.20
	12.72	0.0176	–0.0165	–0.0206	–0.0247	–0.0323	–0.0364	–0.0406	–0.0364	
FL1NW	12.68	0.0159	0.0127	0.0159	0.0201	0.0303	0.0335	0.0367	0.0335	0.20
	12.72	0.0159	0.0165	0.0253	0.0304	0.0379	0.0429	0.0480	0.0429	
FL2NE	12.68	0.0176	–0.0106	–0.0162	–0.0194	–0.0288	–0.0321	–0.0353	–0.0321	0.20
	12.72	0.0176	–0.0203	–0.0242	–0.0290	–0.0352	–0.0400	–0.0448	–0.0400	
FL2NW	12.68	0.0159	0.0171	0.0214	0.0257	0.0347	0.0390	0.0432	0.0390	0.20
	12.72	0.0159	0.0242	0.0303	0.0364	0.0418	0.0479	0.0539	0.0479	
FL1SE	12.68	0.0176	–0.0154	–0.0192	–0.0231	–0.0312	–0.0351	–0.0389	–0.0351	0.20
	12.72	0.0176	–0.0208	–0.0260	–0.0312	–0.0366	–0.0419	–0.0471	–0.0419	
FL1SW	12.68	0.0159	0.0039	0.0065	0.0098	0.0215	0.0241	0.0274	0.0241	0.20
	12.72	0.0159	0.0045	0.0076	0.0113	0.0221	0.0252	0.0289	0.0252	

Note: $\phi = 1$.

*Slab rotations on either side of connection were averaged.

†Note that punching capacity is at least this drift level.

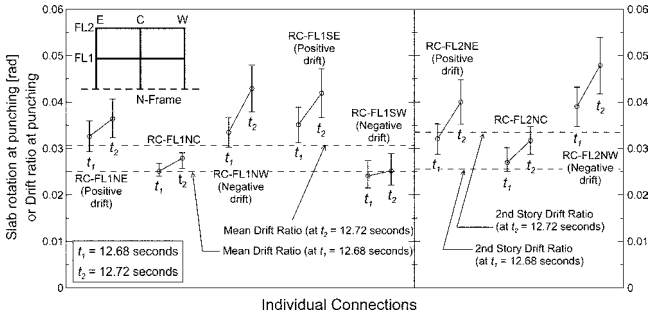

Fig. 6—Slab rotation capacities at punching of individual connections (reinforced concrete specimen).

elastic (θ_y) and plastic (θ_{pl}) rotations. Elastic rotations were computed based on the calculated slab yield curvature ϕ_y and stiffness (M_y/ϕ_y) and an assumed inflection point at slab midspan, whereas plastic rotations were determined by integrating average slab plastic curvatures determined from displacement sensors (LVDTs) mounted on the slab adjacent to the slab-column connections. The displacement readings for each sensor were divided by the sensor gauge length to obtain average strain, and the average curvature was obtained by dividing the average strain readings for sensors on the top and bottom faces of the slab by the distance between the sensors. Results obtained using the two approaches were reasonably close, as shown in Fig. 6, and are discussed in the following sections. Additional details concerning the tests and the data reduction are provided by Kang.[19]

Reinforced concrete specimen—interior connections

Figure 7 features slab curvature versus column curvature diagrams on either side of a roof interior connection (RC-FL2NC), where average curvatures were derived from displacement gauges embedded into the slab (or column) adjacent to the column (or slab). Although strength degradation is noted for RC-FL2NC-w (Fig. 7(a)), K_1 = 0.751 (t = 14.38 seconds) degrades to K_2 = 0.433 (t = 28.04 seconds), only modest degradation is noted for other cases (that is, negative bending for RC-FL2NC-w or RC-FL2NC-e; Fig. 7(a) and (b)). The data for slab curvature obtained from reinforcing bar strain gauges also indicate that yielding of slab reinforcement occurred at the second-story interior connections (Fig. 7(c)). The data indicate that yielding of slab reinforcement occurred, but that punching failures probably did not occur at the interior roof level connections.

Based on the plot of slab curvature on the west side of the connection versus column curvature for the column extending below the slab (Fig. 7(d)). It is concluded that the first-story interior connection (RC-FL1NC) experienced punching failure at approximately t = 12.68 seconds. The ratio of column to slab curvature was significantly lower after t = 12.68 seconds for both positive and negative bending. In addition, the column curvatures (or moment transfer capacity) were reduced to approximately 1/3 of the peak values at the slab curvatures of ±0.0013/cm, suggesting a substantial drop in the column moment.

The drift ratio at punching was obtained using the same two approaches outlined previously for the RC exterior connections, with results shown in Fig. 6 and Table 4 and 5. Figure 6 indicates that the slab rotations at punching (or maximum values, if punching was not observed) range between 0.024 and 0.037 radians (average value = 0.028 radians) for the interior connections and 0.022 and 0.054 radians (average value = 0.036 radians) for the exterior connections (Table 5). In general, because lower gravity shear ratios exist for the exterior connections, the slab rotations at punching for the exterior connections tend to be greater than those for the interior connections, except for the RC-

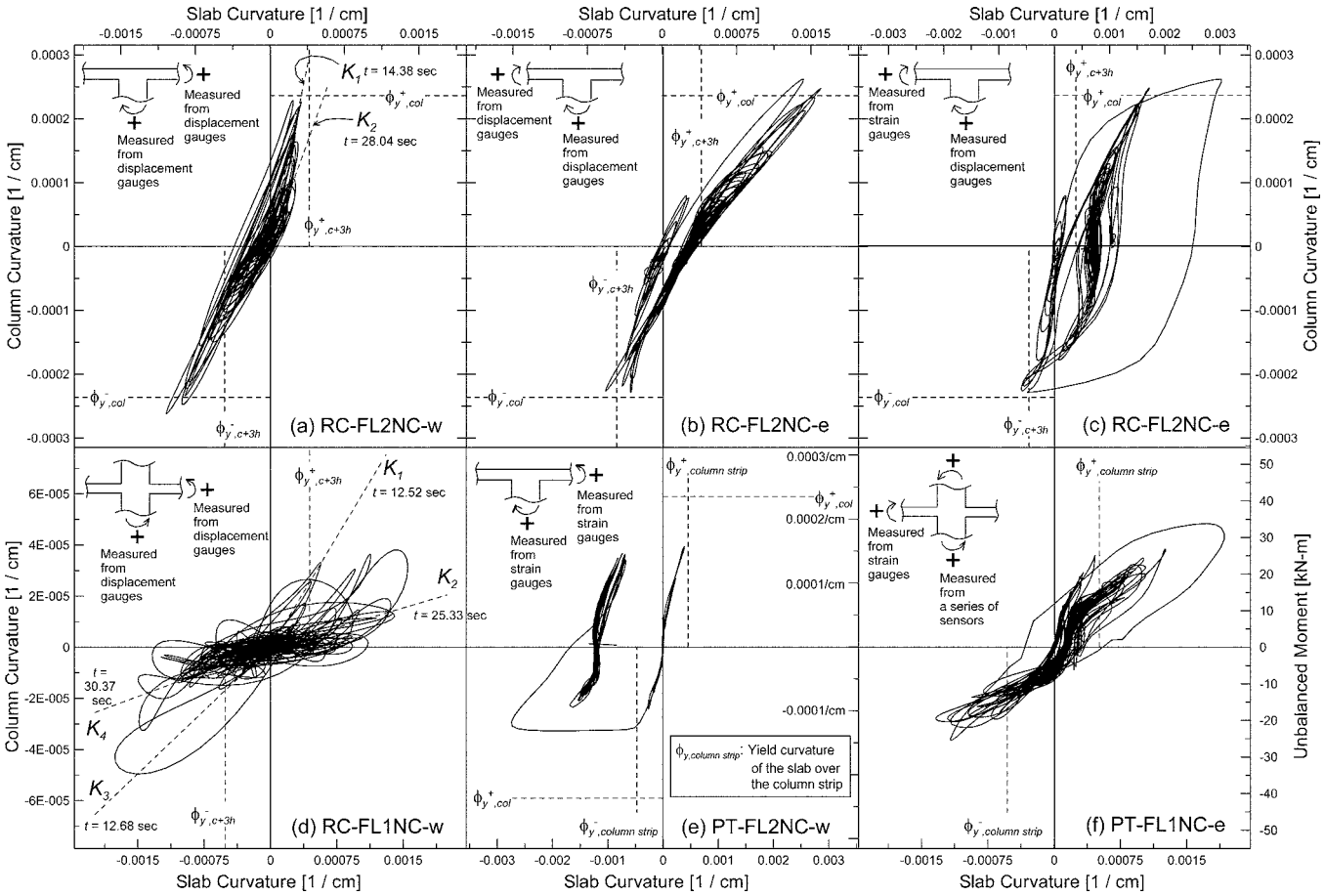

Fig. 7—Slab curvature versus column curvature (reinforced concrete and post-tensioned interior connections).

FL1SW connection (Fig. 6). Results for average interstory drift at punching also are shown on Fig. 6 and indicate values between 0.025 and 0.031 for the first-floor connections and between 0.025 and 0.034 for the roof level connections (Table 4). The values obtained using the rotations (Table 5) and drift (Table 4) are reasonably consistent; however, when using drift ratios, it is not possible to distinguish between interior and exterior connections.

Post-tensioned specimen—interior connections

Figure 7(e) and (f) features column and slab curvature data obtained from reinforcing bar strain gauges for interior connections. Significant yielding without degradation was observed for both positive and negative bending for the roof level connections (Fig. 7(e)), indicating that punching failures did not occur. This is consistent with the yield lines that were observed to extend along the full slab width.[12,19]

For the first-story interior connection (PT-FL1NC), the unbalanced moments were derived from column reinforcing bar strain gauge data at the top of the second-story column (and a computed M-ϕ relation), triaxial load cell data at the base of the first story column, and floor acceleration data.[19] Although results indicate a drop in stiffness after the cycle to peak unbalanced moment (Fig. 7(f)), apparently due to yielding of slab bonded reinforcement followed by deterioration of the shear strength at the interface between the column and the slab (based on observations from video), no significant drop in unbalanced moments could be ascertained. This is likely due to the presence of the unbonded post-tensioning reinforcement, which remains elastic due to the long unbonded length. Based on these findings, as well as the lack of quality slab curvature data at other connections, slab rotations at punching could not be derived for the individual connections of the PT specimen. Therefore, punching failures were assessed using story shear versus interstory drift relations (Fig. 5). Based on a 35% loss of the base shear capacity from the peak value to the residual base shear associated with the column capacity, lateral drift ratios at punching were found to be varying between 2.8 to 4.3% (average value = 3.4%), for the first-story and roof connections, respectively (Fig. 5; Table 4).

DRIFT CAPACITY AT PUNCHING VERSUS GRAVITY SHEAR RATIO

Relationships for drift capacity at punching versus gravity shear ratio have been derived for reinforced concrete specimens without (for example, Pan and Moehle[2,4]) and with stud-rails (for example, Robertson et al.[10]). The results obtained for the shaketable tests described herein are compared with results assembled from existing tests of reinforced concrete or PT slab-column connections, with and without shear reinforcement, to assess whether existing trends adequately represent the results for the dynamic tests of the RC and PT specimens with shear reinforcement. The data plotted are based on actual material properties and for a capacity reduction factor $\phi = 1$. Several significant trends are apparent in the results presented in Fig. 2 and 8.

For RC connections without shear reinforcement (Fig. 8), a very clear trend exists, with a drop in the drift capacity at punching as the gravity shear ratio increases. Results for the

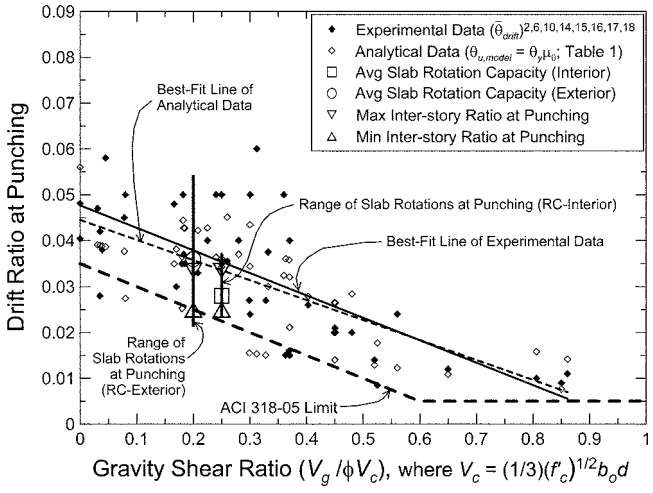

Fig. 8—Drift ratio at punching versus gravity shear ratio (reinforced concrete interior connections without shear reinforcement and reinforced concrete shaketable specimen).

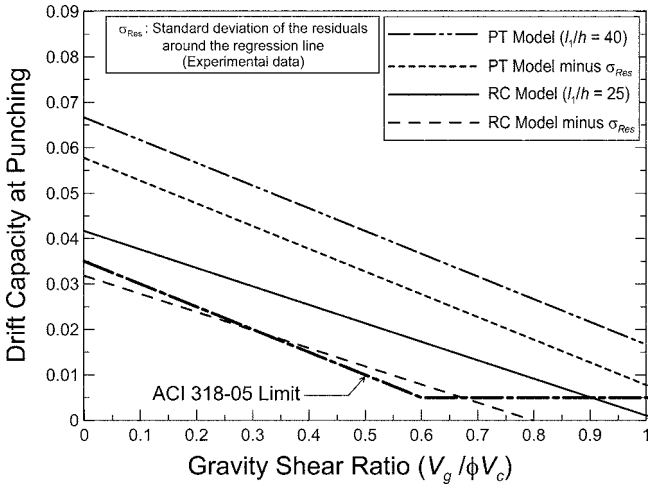

Fig. 9—Predicted drift capacities at punching of reinforced concrete and post-tensioned slab-column connections.

exterior connections of the RC shaketable specimen (Fig. 8), which included shear reinforcement, have approximately the same average value and range as tests of the interior connections without shear reinforcement, whereas the mean and range for the RC shaketable specimen interior connections (Fig. 8), which included shear reinforcement, are slightly lower than reported for previous tests. In addition, as noted previously using the data plotted on Fig. 2(a), the limited test results for isolated exterior connections are consistent with the trend line for interior connections.

For PT slab-column connections, the drift capacity at punching is also strongly influenced by the gravity shear ratio, as shown in Fig. 2(c). The influence of gravity shear is clearly evident for specimens tested within a specific tests program (for example, for the tests by Trongtham and Hawkins,[23] Foutch et al.,[24]and Qaisrani[11]). The trend line in Fig. 2(c) was derived from the database of existing test results (19 specimens) for isolated PT specimens without shear reinforcement. The results presented tend to show more scatter than the tests conducted on the RC specimens, which might be due to the range of loading conditions for the PT specimens (monotonic to reversed cyclic) (Table 3; Fig. 2(c)). The trend line for the eight PT specimens subjected to reversed cyclic loads results in significantly lower drift estimates at punching. Higher drift values at punching were obtained for the PT slab-column connections compared with those for the RC slab-column connections, especially for the connections with large gravity shear ratios; however, it is noted that PT systems tend to be more flexible due to the larger slab span-to-thickness ratios. The range of results obtained for the PT shaketable specimen (Table 4) is consistent with the trend and scatter obtained from previous tests as indicated in Table 3, especially for the previous tests for reversed cyclic loading.

Results for tests of RC slab-column connections with shear reinforcement are plotted in Fig. 2(b) and indicate that the drift capacities of isolated specimens tested under quasi-static, cyclic displacement histories are substantially greater where shear reinforcement is used (for example, Dilger and Brown[14]). However, drift ratios at punching derived from the shaketable tests described in this paper are substantially less than those obtained in the previous test programs for quasi-static loadings. Potential reasons for these discrepancies are discussed in the following paragraphs.

Previous tests were conducted almost exclusively on isolated slab-column specimens, whereas the shaketable studies were conducted on a two-bay, two-story frame, which would be stiffer due to coupling. For the span-to-thickness ratios used for the specimens, however, the impact of coupling would be minimal. In addition, the test results for a nine-panel, one-story frame test[18] and two-bay, slab-column subassemblies[6] are consistent with trends for the isolated connection tests (Fig. 2(a)). Based on available information, the impact of coupling is not expected to have a significant impact on the drift ratio at punching.

In quasi-static tests, it is fairly common to apply cyclic displacement history to the specimen and hold the test specimen at or near the peak displacement value as cracks and damage are noted and photos taken. Therefore, there is an expectation that the degree and extent of cracking would be more significant for quasi-static tests compared with dynamic tests, where peak displacements occur for only a very short duration. Given this expectation, with all other things being equal, larger drift capacities at punching would be expected for dynamic tests. Although the extent of slab cracking was less widely distributed in the shaketable test compared with quasi-static tests,[19] the drift capacities at punching were substantially less than expected based on previous tests.

Two factors might influence the trends noted in Fig. 2(b), which are inconsistent with the expectations noted in the previous paragraph. First, in the shaketable tests conducted, stud-rail strains were relatively small, that is, the maximum strain of 812 μs (versus a yield strain of 2500 μs) measured in the stud-rails is relatively small, whereas stud-rail yielding was achieved in many of the other tests depicted in Fig. 2(b). This difference is a result of the objectives of the tests. For the shaketable tests, the slab reinforcement was designed to reach yield prior to punching failure (referred to in this paper as a drift-induced versus a stress-induced punching failure [Fig. 1]), whereas some of the other tests (Dilger and Brown[14] and Dilger and Cao[25]) were designed to assess the contribution of the stud-rails to the shear strength by manipulating the test condition (that is, larger slab shear-to-moment ratios and slab reinforcement ratios). Second, observed connection behavior during the shaketable tests (captured on video) suggests that the shear strength at the interface between the

slab and the column deteriorated such that the slab moment transferred to the column was reduced, effectively limiting slab damage and the stud-rail strains. It is likely that this degradation of interface shear capacity would not be captured in quasi-static tests, resulting in different behavior.

Although the drift ratios at punching derived for the RC and PT shaketable specimens with shear reinforcement are close to those obtained from the previous test results of the RC and PT connections without shear reinforcement, respectively, the test results indicate that use of slab shear reinforcement substantially reduces the extent of damage[12,19] and, in particular, prevents the "dropping" of the slab observed in the test specimens where shear reinforcement is not provided. In addition, the level of strength degradation for the shear-reinforced connections does not appear to be as drastic as it is for previous tests, particularly for the PT specimen because of the contribution of the unbonded post-tensioning reinforcement to the moment capacity. In addition, the degree of cracking at the interior connections of the PT specimen with shear reinforcement was limited,[12,19] suggesting that it may be possible to repair the connection at relatively low cost (for example, by epoxy injection). Based on the shaketable test results reported (for example, Fig. 8), the new ACI 318[1] provisions adopted for "Frame members not proportioned to resist forces induced by earthquake motions" to address the issue of punching of slab-column connections, would not appear to prevent some strength degradation for cases where shear reinforcement is required. The degree of strength degradation and damage at the slab-column connections, however, is expected to be substantially reduced relative to expectations for connections without shear reinforcement.

Results for the shaketable test program involved relatively low gravity shear stress ratios at the connections compared with common U.S. practice (because of the dual focus of the research program for both U.S. and Japan practices). Additional tests at higher ratios (for example, 0.4 to 0.6) would be helpful to verify the trends identified for higher gravity shear ratios. It is also noted that the residual (post-punching) moment transfer capacity may be significantly greater (non-zero) for unbonded PT construction relative to RC construction. Based on the results presented herein, additional studies are needed before relations for punching of shear-reinforced connections can be developed, which would be desirable for a performance-based design approach.

SHEAR STRENGTH DEGRADATION MODEL

According to the ACI 318-05[1] Section 21.11.5 provisions, shear reinforcement is not required if the connection design for the design shear and unbalanced moment transferred under the design displacement satisfies Section 11.12.6 (that is, no stress-induced failure). As written, the provision does not address the potential shear-strength degradation that occurs for drift-induced punching failures; therefore, punching failures may still occur. To address this issue, available models for shear strength degradation are reviewed and the slab-column test data are used to develop appropriate relationships for both reinforced concrete and PT concrete slab-column connections.

In 1996, Moehle[5] proposed extending the use of a shear strength degradation model to the evaluation of the drift capacity at punching of slab-column connections. In the approach proposed by Moehle,[5] the story drift is assumed equal to the slab rotation, and the slab rotation is determined as $\theta_{u,model} = \theta_y(\mu_\theta)$, where the yield rotation θ_y is approximated as $\phi_y(l_1)/6 \approx l_1/(2400h)$, and μ_θ is determined from the gravity shear ratio using the shear strength degradation model for the RC bridge columns proposed by Aschheim and Moehle.[26] The model captures the trend observed for tests of 23 isolated RC interior connections and three isolated PT interior connections quite well.[5] These findings are reexamined based on the availability of new data for both slab-column connections, as well as the availability of new shear strength degrading models.

The shear strength degradation model proposed by Aschheim and Moehle[26] is applied to the slab-column connections. The model uses two parameters: the displacement ductility at which the shear strength begins to degrade ($\mu_{\delta,1}$) and the rate at which the shear strength degrades (m). Values for these parameters were determined from the existing test data using a least-squares approach, resulting in $\mu_{\delta,1}$ equal to 1 and m equal to 1/3 for the RC interior connections without shear reinforcement. The model parameters determined for the RC connections without shear reinforcement are quite similar to those ($\mu_{\delta,1} = 1$, $m = 1/3.5$) used for the model for the RC bridge columns proposed by Aschheim and Moehle,[26] indicating use of the expanded database (from the 23 specimens used by Moehle[5] to the 45 specimens listed in Table 1) and the new shear strength degrading model do not significantly impact the overall trends previously reported.

For the RC specimens with shear reinforcement, application of the model to a reduced data set ($l_1/h > 15$) indicated substantial scatter; therefore, reliable results could not be obtained with the model. For PT connections without shear reinforcement, cyclic test results are limited to only eight specimens; however, analysis results for the limited data set indicate the strength degradation trends are similar to those for the RC specimens without shear reinforcement. Therefore, at this time, the relationship for RC specimens without shear reinforcement is applied to both RC and PT connections. Therefore, for both RC and PT connections, the impact of shear strength degradation for drift-induced punching can be assessed using the proposed model.

Using the proposed shear strength degradation model, along with typical slab span-to-thickness ratios for RC ($l_1/h = 25$) and PT ($l_1/h = 40$) construction, alternative relationships for assessing the need for shear reinforcement at slab-column connections for RC and PT construction are developed (for example, similar to the relation used in ACI 318-05[1]). The (l_1/h) ratios and $V_g/\phi V_c$ ratios are used to estimate θ_y and μ_θ, respectively, and $\theta_{u,model} = \theta_y(\mu_\theta)$, as discussed previously. Finally, the story drift ratio is assumed to be equal to the story rotation. Results obtained using this approach are presented in Fig. 9 and indicate that drift capacities at punching for PT connections are substantially larger than for RC connections, primarily due to greater span-to-thickness ratios for PT connections. Results presented allow shear strength degradation to be incorporated and also address the differences between RC and PT systems. These findings are useful for both design of new construction (for example, assessing the potential for punching and the need for shear reinforcement for nonparticipating systems for deformation compatibility), as well as evaluation of slab-column connections for existing construction.

SUMMARY AND CONCLUSIONS

A detailed review of the influence of gravity loads on lateral drift levels at punching were conducted for the two

shaketable test specimens, as well as for previous tests of 95 reinforced and PT concrete slab-column connections. For the two shaketable specimens, based on the observed degradation of the story shear versus interstory displacement relationships, interstory drift ratios at punching ranged between 0.025 and 0.034 for the RC specimen, and between 0.028 to 0.043 for the PT specimen. Slab rotation capacities at punching for the individual connections of the RC specimen were determined by examining when the unbalanced moment transferred at a connection dropped. The averages and ranges of the rotation values obtained by the two approaches are reasonably consistent.

Results for the shaketable tests conducted indicate substantially less drift ratio at punching than for previous tests of isolated connections with shear reinforcement, possibly due to the lower strain demands on the shear reinforcement and the rotation of the slab-column connection due to the apparent loss of interface shear capacity. However, the degree of damage and strength degradation expected for connections with shear reinforcement is substantially less than expected for connections without shear reinforcement.

The drift capacity model of the slab-column connections proposed by Moehle[5] was reexamined based on the existing test data and available shear strength degradation models. The revised model addresses the impact of shear strength degradation on drift-induced punching failures and also provides an approach to assess the need for slab shear reinforcement that differentiates between RC and PT connections; both of these issues are not addressed in ACI 318-05.[1]

ACKNOWLEDGMENTS

The work presented in this paper was sponsored by Phase IV of the joint Consortium of Universities for Research in Earthquake Engineering (CUREE)—Kajima Research Program. The authors would like to acknowledge K. Igarashi and N. Suzuki at Kajima Corp., as well as J. P. Moehle, D. Cylde, and W. Neighbour at the Earthquake Engineering Research Center for their support and advice. The views expressed are those of the authors and do not necessarily represent those of the sponsor.

NOTATION

b_o = perimeter of critical section
c = diameter from centroid of critical section to perimeter critical section
d = effective section depth
J_c = property of assumed critical section analogous to polar moment of inertia
l_1 = slab span length between column supports in the direction of lateral loading
V_c = nominal concrete shear strength according to ACI 318-05, Section 11.12.2
V_g = gravity shear force transferred from slabs to column
V_u = applied shear force on critical section
μ_θ = ductility determined based on shear strength degradation model
$\theta_{u,model}$ = drift ratio at punching predicted based on shear strength degradation model
θ_y = yield rotation
θ_{drift} = drift ratio at punching obtained from test results

REFERENCES

1. ACI Committee 318, "Building Code Requirements for Structural Concrete (ACI 318-05) and Commentary (318R-05)," American Concrete Institute, Farmington Hills, Mich., 2005, 430 pp.

2. Pan, A. D., and Moehle, J. P., "Lateral Displacement Ductility of Reinforced Concrete Flat Plates," *ACI Structural Journal*, V. 86, No. 3, May-June 1989, pp. 250-258.

3. Hawkins, N. M., and Mitchell, D., "Progressive Collapse of Flat Plate Structures," ACI JOURNAL, *Proceedings* V. 76, No. 7, July 1979, pp. 775-808.

4. Pan, A. D., and Moehle, J. P., "An Experimental Study of Slab-Column Connections," *ACI Structural Journal*, V. 89, No. 6, Nov.-Dec. 1992, pp. 626-638.

5. Moehle, J. P., "Seismic Design Considerations for Flat-Plate Construction," *Mete A. Sozen Symposium: A Tribute from His Students*, SP-162, J. K. Wight and M. E. Kreger, eds., American Concrete Institute, Farmington Hills, Mich., 1996, 460 pp.

6. Robertson, I. N., and Durrani, A. J., "Seismic Response of Connections in Indeterminate Flat-Slab Subassemblies," *Report* No. 41, Department of Civil Engineering, Rice University, Houston, Tex., 1990, 266 pp.

7. ACI Committee 318, "Building Code Requirements for Structural Concrete (ACI 318-02) and Commentary (318R-02)," American Concrete Institute, Farmington Hills, Mich., 2002, 443 pp.

8. Megally, S. H., and Ghali, A., "Design Considerations for Slab-Column Connections in Seismic Zones," *ACI Structural Journal*, V. 91, No. 3, May-June 1994, pp. 303-314.

9. Megally, S. H., "Punching Shear Resistance of Concrete Slabs to Gravity and Earthquake Forces," PhD thesis, Department of Civil Engineering, University of Calgary, Calgary, Alberta, Canada, 1998, 468 pp.

10. Robertson, I. N.; Kawai, T.; Lee, J.; and Enomoto, B., "Cyclic Testing of Slab-Column Connections with Shear Reinforcement," *ACI Structural Journal*, V. 99, No. 5, Sept.-Oct. 2002, pp. 605-613.

11. Qaisrani, A.-N., "Interior Post-Tensioned Flat-Plate Connections Subjected to Vertical and Biaxial Lateral Loading," PhD thesis, Department of Civil Engineering, University of California-Berkeley, Berkeley, Calif., 1993, 303 pp.

12. Kang, T. H.-K., and Wallace, J. W., "Dynamic Responses of Flat Plate Systems with Shear Reinforcement," *ACI Structural Journal*, V. 102, No. 5, Sept.-Oct. 2005, pp. 763-773.

13. Hawkins, N. M.; Mitchell, D.; and Sheu, M. S., "Cyclic Behavior of Six Reinforced Concrete Slab-Column Specimens Transferring Moment and Shear," *Progress Report* 1973-74 on NSF Project GI-38717, Section II, Department of Civil Engineering, University of Washington-Seattle, Seattle, Wash., 1974, pp. 306-315.

14. Dilger, W. H., and Brown, S. J., "Earthquake Resistance of Slab Column Connections," *Proceedings of Canadian Society of Civil Engineering Conference*, V. 2, Winnipeg, Canada, 1994, pp. 388-397.

15. Luo, Y. H., and Durrani, A. J., "Equivalent Beam Model for Flat-Slab Buildings—Part I: Interior Connections," *ACI Structural Journal*, V. 92, No. 1, Jan.-Feb. 1995, pp. 115-124.

16. Hueste, M. B. D., and Wight, J. K., "Nonlinear Punching Shear Failure Model for Interior Slab-Column Connections," *Journal of Structural Engineering*, ASCE, V. 125, No. 9, Sept. 1999, pp. 997-1008.

17. Robertson, I., and Johnson, G., "Cyclic Lateral Loading of Nonductile Slab-Column Connections," *ACI Structural Journal*, V. 103, No. 3, May-June 2006, pp. 356-364.

18. Hwang, S. J., and Moehle, J. P., "Vertical and Lateral Load Tests of Nine-Panel Flat-Plate Frame," *ACI Structural Journal*, V. 97, No.1, Jan.-Feb. 2000, pp. 193-203.

19. Kang, T. H.-K., "Shake Table Tests and Analytical Studies of Reinforced and Post-Tensioned Concrete Flat Plate Frames," PhD thesis, Department of Civil and Environmental Engineering, University of California, Los Angeles, Calif., 2004, 309 pp.

20. Moehle, J. P., and Diebold, J. W., "Experimental Study of the Seismic Response of a Two-Story Flat-Plate Structure," *Report* No. UCB/EERC-84/08, Earthquake Engineering Research Center, University of California, Berkeley, Calif., 1984, 244 pp.

21. Hayes, J. R.; Foutch, D. A.; and Wood, S. L., "Influence of Viscoelastic Dampers on the Seismic Response of a Lightly Reinforced Concrete Flat Slab Structure," *Earthquake Spectra*, V. 15, No. 4, Nov. 1999, pp. 681-710.

22. PEER Strong Motion Database, Pacific Earthquake Engineering Research Center, University of California-Berkeley, Berkeley, Calif.

23. Trongtham, N., and Hawkins, N. M., "Moment Transfer to Columns in Unbonded Post-Tensioned Prestressed Concrete Slabs," *Report* SM77-3, Department of Civil Engineering, University of Washington-Seattle, Seattle, Wash., 1977, 186 pp.

24. Foutch, D. A.; Gamble, W. L.; and Sunidja, H., "Tests of Post-Tensioned Concrete Slab-Edge Column Connections," *ACI Structural Journal*, V. 87, No. 2, Mar.-Apr. 1990, pp. 167-179.

25. Dilger, W. H. and Cao, H., "Behavior of Slab-Column Connections Under Reversed Cyclic Loading," *Proceedings*, 5th International Colloquium on Concrete, Cairo, 1994, pp. 595-606.

26. Aschheim, M., and Moehle, J. P., "Shear Strength and Deformability of RC Bridge Columns Subjected to Inelastic Cyclic Displacements," *Report* No. UCB/EERC 92/04, Earthquake Engineering Research Center, University of California-Berkeley, Berkeley, Calif., 1992, 99 pp.

Disc. 103-S56/From the July-Aug. 2006 *ACI Structural Journal*, p. 531

Punching of Reinforced and Post-Tensioned Concrete Slab-Column Connections. Paper by Thomas H.-K. Kang and John W. Wallace

Discussion by Robert E. Englekirk

Englekirk Partners Consulting Structural Engineers, Inc., Los Angeles, Calif.

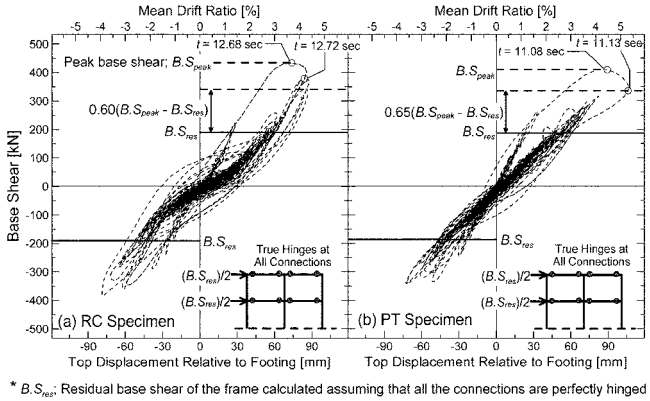

Fig. A—Base shear versus mean drift ratio.

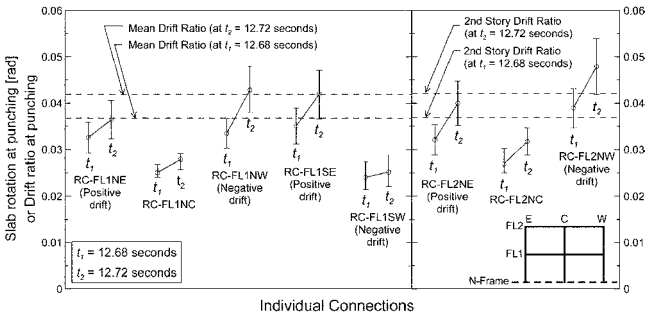

Fig. B—Slab rotation capacities at punching of individual connections (reinforced concrete specimen).

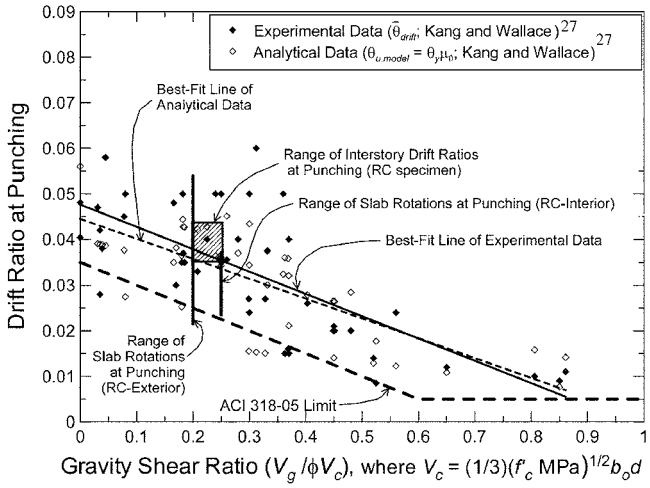

Fig. C—Drift ratio at punching versus gravity shear ratio (reinforced concrete interior connections without shear reinforcement and reinforced concrete shaketable specimen).

This article is in support of ACI 318-05, Section 21.11.5. It suggests that the identified limit states (Fig. R21.11.5) are quite conservative. The discusser raises four questions for the authors.

Question 1—Figures 2(a) and 8 identify V_c as $(1/3)f'_c{}^{1/2}b_o d$. The ACI limit state for slab shear V_c is slightly more than $2f'_c{}^{1/2}b_o d$. Please explain.

Question 2—Drift limits contained in the ACI 318-05 referenced codes are collapse threshold events. Is a punching shear failure consistent with this design objective?

Question 3—Did any of the referenced test specimens result in a collapse or complete failure of the slab?

Question 4—If the designer of a post-tensioned deck provides shear reinforcement, must he or she still pass at least two strands through the column?

Comment—The cost and time required to build concrete residential buildings has doubled in the last 10 years—compliance with this provision adds another 5%.

AUTHORS' CLOSURE

The authors would like to thank the discusser for his interest in the paper and the opportunity to clarify and comment on the issues raised. In addition, the authors use this opportunity to correct an error in data reduction that impacts the results presented in the paper. Responses to the questions and comments posed by the discusser are provided, followed by the correction.

First of all, the authors would like to clarify that the article was neither for nor against the provisions of Section 21.11.5 of ACI 318-05. Rather, the article provided background, data, and analysis to assess the impact of the provisions as well as to provide context.

In response to Question 1, the authors note that the units used for f'_c are MPa, not psi, and slab shear stress (in psi) for a square critical section is typically $4\sqrt{f'_c}$ psi, not $2\sqrt{f'_c}$ psi. Therefore, the 1/3 multiplier in this case is equivalent to ($0.33\sqrt{f'_c}$ MPa = $4\sqrt{f'_c}$ psi).

In response to Questions 2 and 3, the intent of the ACI 318-05, Section 21.11.5, requirements is to reduce the likelihood of punching failure (damage) in the design-basis earthquake (DBE), and not the maximum considered earthquake, which is generally associated with collapse. As well, at least two continuous bottom bars are required to pass within the column (Section 13.3.8.5) to support gravity load after punching failure. Therefore, the requirements appear to be focused more on improved performance under the DBE versus collapse prevention. The apparent focus on improved performance produced substantial debate within ACI Committee 318 prior to the approval of this code change; however, consensus was apparently achieved because the provision provides both improved performance and safety at relatively low cost.

The shaketable specimens tested by the authors were designed according to the ACI 318-02 code, and thus included continuous bottom (integrity) reinforcement; therefore, no collapse was observed during the tests. Furthermore, allowing complete collapse is not feasible for shaketable tests. Of the prior, quasi-static, lateral load tests referenced, the drift levels at punching failures (that is, substantial loss of lateral load capacity) are reported. None of the tests produced complete collapse, either because testing was stopped or continuous bottom reinforcement was provided to prevent complete collapse.

Table A—Interstory drift capacities at punching

	Time, seconds	$V_s/\phi V_c$	$\overline{\theta}_{drift}$
Reinforced concrete mean drift	12.68	0.25	0.0368
	12.72	0.25	0.0419
Reinforced concrete second-story drift	12.68	0.25	0.0369
	12.72	0.25	0.0421
Post-tensioned mean drift	11.08	0.33	0.0439
	11.13	0.33	0.0521
Post-tensioned second-story drift	11.08	0.33	0.0458
	11.13	0.33	0.0559

Note: $\phi = 1$.

In reference to Question 4, the use of shear reinforcement reduces the extent of the damage and, in particular, prevents the dropping of the slab observed in reinforced concrete connections where shear reinforcement is not provided.[12] Because the shear reinforcement commonly used in construction practice does not pass through the column, it may not be effective in preventing collapse and continued use of current requirements is prudent. The lack of slab damage adjacent to the column could improve gravity load transfer (for example, improved dowel action), however, potentially reducing the quantity of reinforcement that must pass within the column core.

During data reduction, the authors mistakenly removed the contribution of rigid body rotation of the load cells mounted under the footings to the story drift ratio, which impacted Fig. 5, 6, and 8 and Table 4, but not the findings. The corrected figures and table are provided as Fig. A, B, and C and Table A, respectively.

REFERENCE

27. Kang, T. H.-K., and Wallace, J. W., Punching of Reinforced and Post-Tensioned Concrete Slab-Column Connections," *ACI Structural Journal*, V. 103, No. 4, July-Aug. 2006, pp. 531-540.

Disc. 103-S57/From the July-Aug. 2006 *ACI Structural Journal*, p. 541

Design for Shear Based on Loading Conditions. Paper by Michael D. Brown, Oguzhan Bayrak, and James O. Jirsa

Discussion by Himat T. Solanki

ACI member, Professional Engineer, Building Department, Sarasota County Government, Sarasota, Fla.

The authors have presented an interesting paper. The discusser would like to offer the following comments:

1. Based on the cited references by the authors, it appears that the authors are either unaware of the previously published work or may not have reviewed the work.[54-56]

2. Based on the cited references it appears that the authors have not considered the beams such as I-beams, double T-beams with symmetrical and unsymmetrical flange width, beams having an opening(s) within the web (beams having hole(s)), variable (tapered/hunched) depth, or circular beams in their study. Though these beams would not make any difference in the ACI code limitation, they do have an impact on their strength ratio, that is, test values versus calculated values.

3. From the paper, it is very difficult to judge how the analysis (strut-ties model [STM]) was performed, particularly for single-point/two-point/uniformly-distributed loads. For example, in a beam having a single-point concentrated load, was an STM considered as a one-unit truss or a multi-unit truss? (Based on the space truss theory, the STM could be rearranged for a given loading condition.) Though a single-truss versus multi-truss model has no impact on its ultimate load-carrying capacity, it does have an impact on the crack pattern (that is, crack width and crack spacing).

4. The authors have not addressed the crack pattern such as the crack width in their analysis. For example, when all parameters of beams were kept constant, but only the stirrup spacing had changed, what impact would there be on the beam behavior? Borischanskij[57] has tested two beams (Fig. A) with a change in stirrup spacing, and he observed different crack widths for a given load on both beams. From Fig. A, it can be seen that the crack width increases with the stirrup spacing increases for a given constant load condition.

5. As shown in Fig. B, the discusser has analyzed 2381 test specimens, including a large number of the authors' specimens (except References 25, 27, 39, and 47) and also beams such as I-beams, double T-beams with symmetrical and unsymmetrical flange width, beams having an opening(s) within the

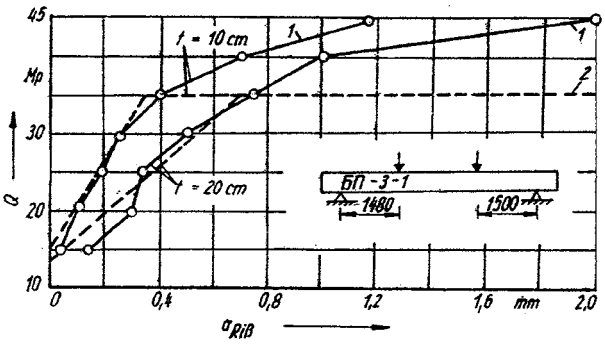

1 Versuche von M. S. Borischanskij
2 Rechnung

			Längsbewehrung			Querbewehrung			
b cm	d cm	R kp/cm²	Anzahl ∅	σ_s kp/cm²	μ_e %	Anzahl ∅	σ_s kp/cm²	t cm	μ_{eB} %
23	62,5	344	8∅25	6 000	2,73	4∅7,9 2∅7,9	3 240	20 10	0,425

Fig. A—Load versus crack width.[57]

web (beam having hole(s)), variable (tapered/hunched) depth, circular beams from various publications using an STM, as well as considering multi-unit truss elements[58,59] for single-point and two-point loading conditions found to be consistent with Hedman and Losberg.[54] These beams were described by the original authors as having a shear failure mode.

6. Because the authors have concentrated on the ACI code formula and its limitation for V_c, the discusser would like to request a clarification based on the following concept:

To calculate the real shear strength of concrete

$$f'_c = P_u/\{A_s\} \quad \text{or} \quad P_u = f'_c A_s$$
$$P_u = 2D^2 f'_c \quad \text{or} \quad P_u = 72 f'_c \tag{5}$$

where P_u equals the failure axial load on cylinder; D equals the diameter of a cylinder equal to 6.0 in. (152.4 mm) (ACI code); and A_s equals the real single plane maximum sheared cross section (maximum probable value of ideal sheared cross section).

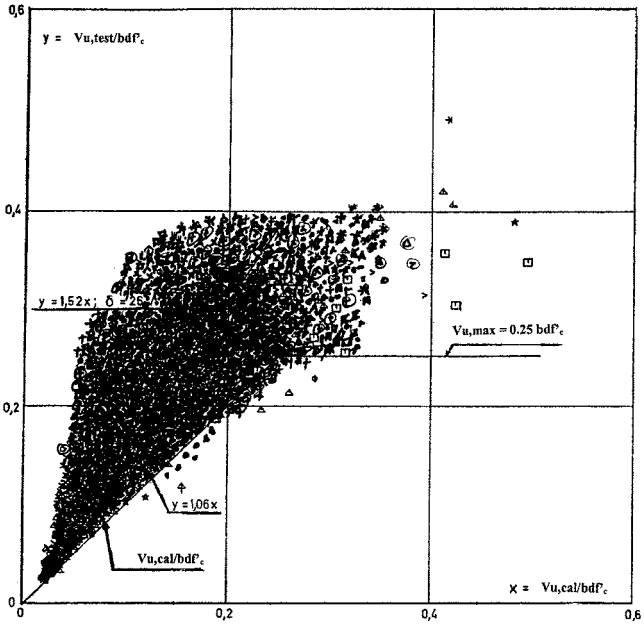

Fig. B—Test shear failure $V_{u,test}$ *compared with calculated shear capacity* $V_{u,cal}$.[54]

Because of the shear strength due to a single concentrated load in the beam along the line of 45 degrees, the shear strength per Joint ACI-ASCE Committee 326[1] and ACI Committee 318[2]

$$v_c = (P_u \text{ or } V_u/2)/bd = 2\sqrt{f_c'}$$
$$\text{or } P_u = 2\sqrt{f_c'}bd \tag{6}$$

Equating Eq. (5) and (6)

$$72 f'_c = 2\sqrt{f_c'}bd$$
$$bd = 36\sqrt{f_c'}$$

or cross-sectional area of beam = $36\sqrt{f_c'}$

This means the cross-sectional area is directly proportional to the square root of the concrete compressive strength and, hence, the square root of the concrete compressive strength controls the beam dimensions/geometries. Is this true? If it is true, how can a dimension for all other beam geometries be established? Should it be based on concrete compressive stress block?

ACKNOWLEDGMENTS

The discusser gratefully acknowledges S. Unjoh, Leader, Earthquake Engineering Team, Public Works Research Institute; R. K. Dhir, University of Dundee; K. Reineck, University of Stuttgart; P. Chanda, British Cement Association; J. Clarke, The Concrete Society; M. W. Braestrup, Ramboll Hannermann Hojlund; R. Heffernan, Institution of Civil Engineers; R. Thomas, Institution of Structural Engineers; and G. Sabnis for providing the publications related to the shear strength of beams.

REFERENCES

54. Hedman, O., and Losberg, A., "Dimensionering av betongkonstruktioner med hänsyn till trärkrafter," *Nordisk Betong*, No. 5, 1975, pp. 19-29.

55. Kordina, K., and Blume, F., "Empirische Zusammenhänge zur Ermittlung Der Schubtragfähigkeit stabförmiger Stahlbetonelemete," No. 364, Deutscher Ausschuss für Stahbeton, Ernst & Sohn, Berlin, Germany, 1985.

56. Walsh, P. F., "Analysis of Concrete Beams Shear test Data," *Report* No. 9, Division of Building Research, Commonwealth Scientific and Industrial Organization, Victoria, Australia, 1973.

57. Salesow, A. S., and IIjin, O. F., "Zur Berechnung von Schrägrissen in Stahlbetoelementen," *Bauplanung—Bautechnik*, V. 29, No. 11, Nov. 1975, pp. 556-560.

58. Ritter, W., "Die Bauweise Hennebique," *Schweizerische Bauzeitung*, V. 33, No. 7, Feb. 1899, pp. 59-61.

59. Mörsch, E., *Der Eisenbetonbau*, Verlag von Konrad Witter, Stuttgart, Germany, 1922.

Disc. 103-S57/From the July-Aug. 2006 *ACI Structural Journal*, p. 541

Design for Shear Based on Loading Conditions. Paper by Michael D. Brown, Oguzhan Bayrak, and James O. Jirsa

Discussion by Ivan M. Viest

ACI member, IMV Consulting, Bethlehem, Pa.

The authors should be congratulated on the significant contribution to shear research. The discusser would like to add a historical perspective.

Equations (1) and (2) are based on research performed at the University of Illinois half a century ago. One of the enduring contributions of that research was expressing the shear strength of concrete as a function of the square root of its compressive strength. In the 1963 issue of the ACI code, the square root relationship replaced an earlier linear one. It has been retained to this day. It first appeared in print in an internal report issued in Dec. 1955 and in the ACI JOURNAL, *Proceedings* in March 1957.[60] In both publications, the shear strength was shown as a function of the ratio of moment to shear in the form M/Vd; and Eq. (2) was suggested as the lower-bound design limit for shear at ultimate load in reinforced concrete members without web reinforcement.

REFERENCES

60. Morrow, J., and Viest, I. M., "Shear Strength of Reinforced Concrete Frame Members without Web Reinforcement," ACI JOURNAL, *Proceedings* V. 53, No. 3, Mar. 1957, pp. 833-869.

Disc. 103-S57/From the July-Aug. 2006 *ACI Structural Journal*, p. 541

Design for Shear Based on Loading Conditions. Paper by Michael D. Brown, Oguzhan Bayrak, and James O. Jirsa

Discussion by Evan C. Bentz

ACI member, Associate Professor, University of Toronto, Toronto, Ontario, Canada.

The authors have presented a paper that makes a case for improving the safety of the shear provisions of the current ACI code. While the discusser fully agrees with this goal, he has serious concerns with the first conclusion presented in the paper. This conclusion is that the shear strength of a member subjected to a uniformly distributed load (UDL) is inherently higher than that of a member subjected to concentrated loads, perhaps twice as high on average. This conclusion is contradicted in previous technical literature and does not appear to be supported by the new tests in the authors' paper. A total of four arguments are used in the paper to support the conclusion and these are each discussed in the following.

The authors note that the current code exempts slabs, footings, and joist construction from the requirement to provide minimum shear reinforcement when the shear exceeds $0.5V_c$. They suggest that this higher allowable stress provides implicit support for their conclusion as these member types are often subjected to uniform loads. It is important to note that the commentary to the code states that these member types "are excluded from the minimum shear reinforcement requirement because there is a possibility of load sharing between weak and strong areas." That is, it indicates a different explanation than that provided by the authors and thus some care is warranted in interpreting any assumed implicit meaning. The technical report on which the current shear strength provisions of the ACI code are based is the "326 Report" from 1962, included in the authors' paper as Reference 1. In this reference, tables show that the average ratio of experimentally-observed shear strength to ACI code predicted shear strength was 1.180 for 430 test results without stirrups. For the subset of 64 experimental results of uniformly loaded members, the average ratio was 1.192. Thus, the report on which the current code provisions are based indicates that the UDL member may be stronger than point-loaded members, but only by approximately 1% on average.

The authors' second argument in favor of their conclusion is in new test results presented on four experiments loaded with a variable number of point loads (refer to Fig. C). The authors suggest that, as the number of point loads is increased on the span, the shear strength increased. Figure D plots the failure shear at the critical section for shear *d* from the support with respect to the distance to the centroid of the forces causing that shear. While there is no clear trend of the shear strength with respect to the loading type, there is a clear trend compared with the shear span. This trend is the same as that shown in Fig. 1 of the authors' paper where Kani showed that shorter shear spans result in higher shear strengths. With regard to this, it is relevant to note that Kani himself, in his 1966 paper on shear,[61] stated that "the behavior of reinforced concrete beams under a uniformly distributed load appears to be essentially the same as under point loads."

The third argument in support of uniformly loaded members being different from point-loaded members is that the distribution of internal concrete strains is different. These results are for members with a shear span-to-depth ratio of 1.0, and thus provide some evidence for behavior associated with an Appendix A strut-and-tie analysis, but their relevance to the "beam shear" equations of Chapter 11, which the authors propose to change, is unclear. Perhaps the authors can explain.

The final argument used is based on the database of shear test results as presented in Table 2 of the paper. The discusser has serious concerns about this comparison primarily due to clear mistakes in the database. Consider that the first data series listed in the table indicates that 54 members were used by the authors, yet the original reference[7] clearly indicates that 18 of these specimens failed in flexure rather than shear. It is not appropriate to compare the ACI shear strength equations with members that did not fail in shear. With a brief examination of Table 2, the reinforcement values for at least seven of the test series were also found to be wrong, often with the lower bound of ρ_w being incorrect by a factor of 10. Overall, the table mixes three failure modes: strut-and-tie failures, beam action shear failures, and flexural failures. These should be compared with the ACI Appendix A strut-and-tie equations, Chapter 11 shear equations, and Chapter 10 flexural equations, respectively. By putting them all together and only comparing them with the simplest shear equation in the

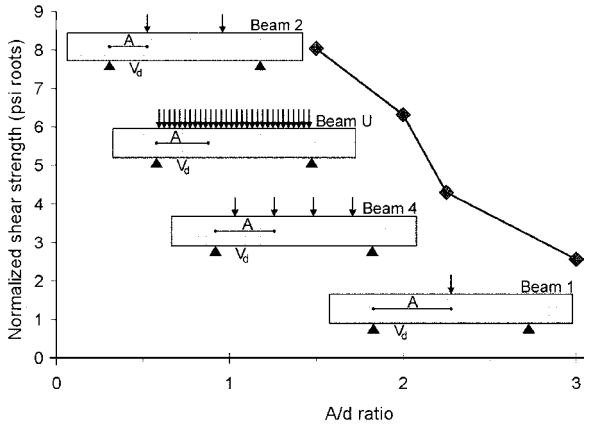

Fig. C—Shear strength of authors' tests with respect to shear span.

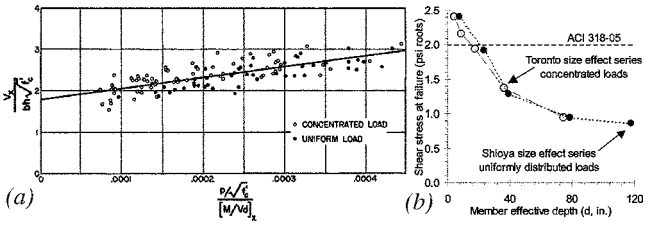

Fig. D—Comparison of shear strengths of uniformly loaded and point loaded members for: (a) small heavily reinforced members; and (b) large lightly reinforced members.

code, it is, perhaps, not surprising that the authors failed to note clear trends in the database.

Conclusions based on Fig. 14 to 22 in the paper should be treated with caution as many make "apples to oranges" comparisons. As an example of an "apples to apples" comparison, Fig. D(a) shows results from tests in the authors' database[17] on UDL and point-loaded members. This clearly shows that small heavily-reinforced beams produce similar shear strengths regardless of loading type. The one set of shear experiments performed to date on uniformly loaded, large lightly-reinforced members is the famous Shioya series from Japan,[23] also included in the authors' database. It appears that the section of text on the bottom half of page 547 in the authors' paper is intended to discredit these tests presumably as they directly refute the authors' conclusions about the safety of uniformly loaded members. These tests were intended to determine the shear strength of the base footing slabs of large in-ground liquid natural gas (LNG) vessels and thus represented members supported on soil. Soil supported structures do not show any shear forces due to self weight and thus it is simply irrelevant that the largest member may not have been able to support its own self weight. Figure D(b) compares these Japanese tests to other tests performed at the University of Toronto, also included in the authors database,[19] in another "apples to apples" comparison. These two experimental series had a similar value of the term $\rho_w Vd/M$, as used in Eq. (1) of the authors' paper and thus the ACI code would suggest that the member should show similar shear behavior. As is clear from the figure, the point-loaded members and the uniformly-loaded members did show very similar behavior. This figure supports the conclusions that: a) the results of the Japanese tests are in no way inconsistent with others and should not be ignored; b) the shear strength of UDL and point-loaded members is essentially the same across different depth ranges; and c) the ACI code has problems with estimating the shear strength of large lightly-reinforced members regardless of loading type.

REFERENCES

61. Kani, G. N. J., "Basic Facts Concerning Shear Failure," ACI JOURNAL, *Proceedings* V. 63, No. 6, June 1966, pp. 675-692.

AUTHORS' CLOSURE

Authors' closure to discussion by Solanki

The discusser provided six specific discussion points. Each is addressed in turn in the following:

1. The authors thank the discusser for calling attention to additional references.[54-56]

2. As stated in the paper, "Some limitations were placed on specimens included in the database. Only rectangular cross sections supported on simple spans, without axial loads, were considered. Normalweight concrete and conventional steel reinforcing bars were used to construct all beams. These limitations were imposed to assure simple, well-defined geometry that would permit relatively easy determination of the concrete contribution to shear strength V_c."

3. The conclusions of this paper are based on and applicable to sectional shear design provisions of ACI 318. The discussion of the experimental results is partially based on strut-and-tie models because strut-and-tie modeling allows the complex behavior of reinforcement concrete elements to be explained in relatively simple terms. No strut-and-tie analyses were presented in this paper.

4. The authors observed that, in general, cracks tend to form at the location of the stirrups. Hence crack spacing was approximately equal to stirrup spacing. If two beams are identical except for the stirrup spacing and are subjected to the same moment, it is likely that fewer, more widely spaced cracks develop in the beam with larger stirrup spacing. Because the beams are subjected to the same curvature, the average bottom fiber strain must be identical; therefore, the beam with greater stirrup spacing could be expected to have larger and more widely spaced cracks than its companion beam with smaller stirrup spacing, as appears to be indicated in the figure showing the work of Borischanskij. However, crack widths were not considered by the authors for the work presented in the paper.

5. The discusser is to be commended for calling attention to test data that extends the data base to include a wide variety of variables not included in the paper or the database used.

6. The authors are unable to follow the derivation for the cross-sectional area of a beam as a function of concrete strength. However, the equation derived indicates that, as the concrete strength increases, the cross-sectional area will also increase. This result does not seem reasonable or consistent with test results or with design practice.

Authors' closure to discussion by Viest

The authors would like to thank the discusser for his kind words regarding the research effort presented in this paper. The authors also thank the discusser for his pioneering research efforts in shear that have endured the test of time since their development 50 years ago.

Authors' closure to discussion by Bentz

The authors wish to thank the discusser for his comments and for his thorough review of the paper. Prior to addressing his concerns, it is important to state the primary goal of the paper which was to ensure that the nominal shear strength a designer determines using the simple expression ($V_c = 2\sqrt{f_c'}\, b_w d$) given in ACI 318-05 provisions can in fact be realized.

The questions posed by the discusser regarding the conclusions will be discussed individually.

Load distribution—In a Bernoulli Beam, a truss consisting of a number of diagonal struts and horizontal and vertical ties may form between the applied loads and supports. For loads that are not far away from the supports (within approximately 2*d*), a direct strut may form between the loads and the support. In both instances, the dispersion of stress through the depth of the member triggers the formation of truss mechanisms through cracking and redistribution of stresses. Figure 11 was intended to graphically depict such redistribution in members subjected to uniform loads as compared with members with distributed loads. In Fig. 11, the distribution of measured strains from a beam subjected to uniform loads is quite different from the distribution associated with a concentrated load. On average, the measured strains from the uniformly loaded beam are much higher than those measured during the concentrated load test. These two strain distributions show clear evidence of stress redistribution. The discusser indicates that slabs, footings, and joist construction are exempt from the minimum shear reinforcement requirements because these types of construction have a significant capacity to redistribute stresses from strong areas to weak areas. As stated in our paper, the authors agree with this statement. Furthermore, the authors suggest that, in the case

of a beam subjected to uniformly distributed load, multiple load paths between the applied load and support exist. With multiple load paths, redistribution is possible. The strain distributions in Fig. 11 show the results of that redistribution. Strain is migrating from the peak value (as shown for the concentrated loads) to a more uniform distribution (as shown for the distributed load).

The discusser also indicates that the 1962 Committee 326 report[1] did not find any difference between concentrated and uniform loads because the average values of ratio of measured to calculated values of shear were within 1% of each other. The discusser's assertion is based on average values. The authors focused solely on the lower-bounds to the data. While on average there may be little difference between concentrated and uniform loads, the lower-bounds of these two types of members are quite different. In data where significant scatter exists, both accuracy and safety cannot be assured simultaneously. An average value of tested to calculated strength of 1.00 indicates that 50% of the test specimens would have a failure load less than the nominal capacity. Such an approach is not appropriate for a design code. Conclusions in the paper are based on a lower-bound to strength rather than the average. Furthermore, the 1962 ACI Committee 326[1] report specifically cited differences in the cracking behavior of beams with concentrated or uniform loads.

Use of small datasets—Establishing trends by passing a line through a small number of data points may result in conclusions that have limited or no use in the development of expressions for design codes. The plot of the authors' data in Fig. C is not correct. The corrected version is show in Fig. E. ACI 318-05, Section 11.1.3c, allows the critical section of a beam to be calculated a distance *d* from the support only if there are no concentrated loads applied within a distance *d* from the support. The authors' Beam 4 does not meet that criterion and, therefore, the shear at the critical section should be twice the value at which the discusser has shown it to be in Fig. C. When plotted in the correct location (Fig. E), the trend described by the discusser is no longer present. Note that the specimen subjected to a single concentrated load has much less shear strength than the remaining three specimens that were subjected to multiple loads. Figures C and E highlight the potential for errors that arises when attempting to base wide-ranging conclusions on only a few data points. For this reason, the authors based all of their conclusions on a combination of their own experimental work and a large database of published work. To reinforce this point, the authors would like to quote from Reineck et al.,[62] "Year by year, different proposals are put forward by researchers all over the world for predicting the shear capacity of members without transverse reinforcement. The proposed relationships are usually empirical and designed to fit the limited set of shear test results that are most familiar to the researcher(s)…This limited amount of information is insufficient for the development of comprehensive and reliable expressions for estimating the shear strength of concrete members."

The discusser has presented a figure from the Committee 326 report in Fig. D(a). Based on this figure, the discusser concludes that there is no significant difference in shear strength based on loading type. Based on the work presented by Leonhardt[63] and Uzel,[25] the authors disagree. Leonhardt reasoned that, in the portion of a beam beneath a load or above a reaction, a vertical stress acts on the beam due to the compression induced by the loads. These vertical stresses reduce the principle tensile stresses in the member. By reducing principle tensile stresses, the external loads or reactions restrain the formation of a diagonal tension crack and shear strength is thereby enhanced. Uzel[25] identified, through both experimental and analytical investigation, the same phenomenon in footings that were subjected to concentrated loads and supported by uniform loads. Uzel described these compressive stresses induced by supports and loads as clamping stresses. In both cases, the beneficial effects of distributed loading were clearly observed and noted.

The discusser included a quote from Kani[61] and the readers should note that in the paragraph following the one from which the discusser quoted, Kani further states that, "A comparison of…point loading tests shows, as could be expected, that a uniformly distributed loading produces somewhat more favorable results. Thus, it is slightly conservative if the design requirements for beams under point loadings are extended to beams under uniform distributed loads." Herein, Kani's language ("…as could be expected…") indicates that he was well aware of a difference between uniform loads and concentrated loads.

The discusser indicated that the Shioya tests were intended to simulate the foundations for LNG tanks and, as such, code provisions that apply to beam designs should not be used to check the validity of those tests. This point is consistent with our impression of the Shioya tests. While they may provide valuable data for certain issues, their use in judging the beam shear or sectional shear provisions of ACI code is not appropriate. After stating that beams cannot be compared with footings due to the way the two types of members handle self-weight, Fig. D(b) is presented to identify parallels between research results from Toronto and research results from Shioya.[23] This would appear to be "comparing apples to oranges."

Shear span-to-depth ratio—The discusser questions the applicability of the specimens shown in Fig. 9 through 11 because these specimens would fall under the strut-and-tie provisions of ACI 318-05. Section 11.8.1 indicates that the ACI 318-05 limits for deep beams where nonlinear strain distributions or strut-and-tie models should be used as a basis for design. Currently, the ACI code suggests the use of strut-and-tie models for members in which the clear span is less than four times the overall depth of the member or if a concentrated is load is located within twice the member depth from the support. Even if a member is considered a deep beam by these provisions, strut-and-tie modeling is not required to design the member.

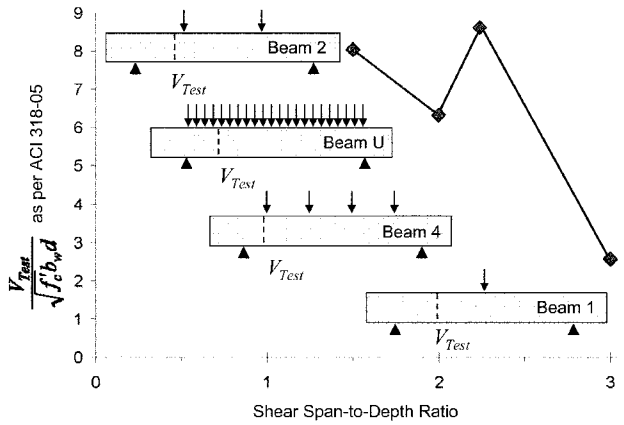

Fig. E—Corrected version of discusser's Fig. C.

The specimen subjected to uniformly distributed loads in this paper has a clear span equal to four times the overall depth and there are no concentrated loads. Hence, these specimens could be designed using the provisions of Chapter 11 of ACI 318-05; although, the authors would recommend the use of Appendix A for such a task. These specimens were included in the paper to highlight the differences in strains for members subjected to concentrated or uniformly distributed loads as per the previous discussion of redistribution.

In his discussion, the discusser indicated that the shear span-to-depth ratio for the specimen subjected to uniform loads over half the span was 1.0. The authors are unsure of the basis for that determination. Additionally, the authors are unsure of the basis for the calculation of shear span for Beam 4 as shown in the discusser's Fig. C. For specimens subjected to multiple loads, or distributed load, the definition of shear span becomes nebulous. Leonhardt and Walther[52] defined the shear span of a uniformly loaded beam as one-fourth of the span length. That decision was made to ensure that the test results from specimens with distributed loads resembled specimens with two concentrated loads. In the process of forcing the two sets of data to resemble one another, Leonhardt and Walther were successful. The definition proposed by Leonhardt and Walther, however, is completely inadequate for specimens such as those presented by the authors (distributed loading over half of the span).

The authors would like to further discuss the definition of shear span by calling attention to the conclusions of Bryant et al.[64] Bryant et al.[64] conducted a series of tests of two-span

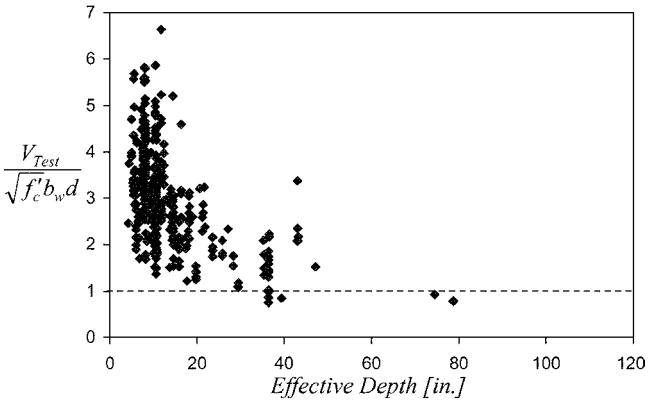

Fig. F—Shear strength versus effective depth based on Reineck et al.[62] database.

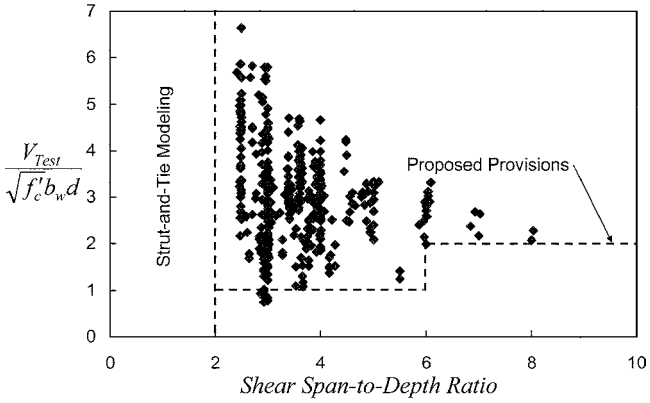

Fig. G—Shear strength versus shear span-to-depth ratio based on Reineck et al.[62] database.

continuous beams with varying numbers of concentrated loads applied to the beams. Those tests consisted of members subjected to 1, 3, 5, or 11 concentrated loads per span. Eleven closely-spaced concentrated loads resemble a uniformly distributed load. Bryant et al. concluded, "As the number of loads on a beam increased, the failure section became impossible to predict. The material and geometrical properties of beam, viz., ρ, f_c', and M/Vd, does not lead to a precise analysis of the failure section for these beams." Note that the quantity M/Vd is equal to the shear span-to-depth ratio. Bryant et al.,[64] therefore, found that the shear span-to-depth ratio is an unreliable parameter for describing the failure of specimens subjected to distributed loadings. So, for specimens subjected to distributed loads, the shear span is difficult to define as evidenced by the inability to define a shear span for the specimen subjected to a partial distributed load but, at the same time, a precise definition may be unnecessary for such specimens based on the conclusions of Bryant et al.[64]

While all data in the shear database assembled during the course of the research is presented in the paper, the only data that is used to arrive at the conclusions that apply to sectional shear provisions of ACI 318 were taken from test specimens with shear span-to-depth ratios greater than two. To be exact, the authors spent a substantial amount of time in studying the potential causes of the low-shear strength values that are limited to a narrow range of shear span-to-depth ratios ($2 < a/d < 6$). All specimens within this shear span-to-depth ratio were thoroughly examined prior to reaching the conclusions reported in the paper.

Shear database—The authors thank the discusser for identifying miscalculations in Table 2. Based on the discusser's comments, the following miscalculations were identified in Table 2:

1. de Cossio and Siess[30]: ρ_w = 1.00 to 3.36%
2. Johnson and Ramirez[15]: ρ_w = 2.49%
3. Kong and Rangan[32]: ρ_w = 1.00 to 4.47%
4. Krefeld and Thurston[17]: ρ_w = 0.80 to 5.01%
5. Ramakrishnan and Ananthanarayana[38]: d = 13.8 to 28.8 in.
6. Rogowsky et al.[21]: ρ_w = 0.90 to 1.12%
7. Roller and Russell[22]: a/d = 1.8 to 2.5
8. Sarsam and Al-Musawi[40]: ρ_w = 2.23 to 3.5%
9. Tan and Lu[43]: ρ_w = 2.60%
10. Xie et al.[50]: ρ_w = 2.07 to 4.54%

It is important to note that these miscalculations were confined solely to the summary table (Table 2) in the paper. The authors have examined the entries corresponding to those miscalculations in the originating database. The values stored in the database and used for analysis within the paper are correct. Therefore, the plots (Fig. 15 through 22) are correct as published. While the authors made every effort to produce a table without errors, some errors did make it through the review process into the final paper. The database that was assembled by the authors is intended to be updated with further developments in shear research. Readers who find errors in the database or test results that are missing are encouraged to contact the authors so that corrections can be made.

In Fig. F and G, the authors have presented data that were assembled as part of another database regarding the shear strength of reinforced concrete beams.[62] In Fig. F, it can be observed that the lower-bound to the data is essentially constant as a function of depth for beams in excess of 30 in. (762 mm). Furthermore, the authors have reproduced Fig. 18 from the original paper using the data collected by

Reineck et al.[62] The results are shown in Fig. G. Regardless of which database is used, the lower-bounds to Fig. 18 and E are essentially the same.

Flexural failure—The discusser has taken issue with the authors' choice to include some specimens in which yielding of flexural reinforcement took place prior to shear failure. In fact, the discusser refers to these specimens as "flexural failure." The authors would like to discuss the subtle, but important, difference between flexural failure and flexural yielding. Flexural yielding involves yielding of the longitudinal reinforcement in tension. Flexural failure involves the loss of equilibrium within a member. Flexural failure is caused by two distinct limit states: crushing of the concrete in the compression zone prior to or after the yielding of longitudinal reinforcement or rupture of the longitudinal reinforcement. Flexural yielding does not in any way imply or require flexural failure. The distinction between flexural yielding and flexural failure is an important one due to the philosophy or ACI 318 and strength design. In all the beams that are designed and detailed according to ACI 318 provisions flexure ought to be the "weakest link" in the chain. In other words, typical beams are designed to possess sufficient shear strength such that flexural yielding and redistribution of the moments takes place prior to shear failure. Throughout the redistribution process, the beams are expected to have sufficient shear strength. The shear strength of a beam that contains large amounts of flexural reinforcement is of limited use to evaluate the performance of beams that are designed using the ACI 318 code.

In short, the ACI 318 code encourages designers to seek ductile limit states (yielding in flexure) rather than brittle ones (shear failure). Therefore, if code documents are predicated on members that fail in shear after yielding in flexure, the code must be based on test specimens with those limit states. Hence, the decision to include members that failed in shear after yielding of the longitudinal reinforcement in the database is consistent with code intent.

In conclusion, researchers have historically favored the use of concentrated loads in tests for shear strength of reinforced concrete beams. Such tests resemble transfer girders more than any other building member. Extrapolating recently reported low shear strengths[19] of elements that are subjected to concentrated loads to beams that support slabs, joists, or other loads that are reasonably uniform should be done with caution. There are no reported instances of shear distress in elements subjected to uniform loads. Once again, we thank the discusser for allowing us to re-evaluate our conclusions and the code change proposal included in our paper through the use of another shear database developed by Reineck et al.[62]

REFERENCES

62. Reineck, K.; Kuchma, D. A.; Kim, K. S.; and Marx, S., "Shear Database for Reinforced Concrete Members Without Shear Reinforcement," *ACI Structural Journal*, V. 100, No. 2, Mar.-Apr. 2003, pp. 240-249.

63. Leonhardt, F., *Prestressed Concrete Design and Construction*, Wilhelm Ernst & Sohn, translated by C. Amerongen, 1964.

64. Bryant, R. H.; Bianchini, A. C.; Rodriguiz, J. J.; and Kesler, C. E., "Shear Strength of Two-Span Continuous Reinforced Concrete Beams with Multiple Points Loading," ACI JOURNAL, *Proceedings* V. 59, No. 9, Sept. 1963. pp. 1143-1178.

Disc. 103-S58/From the July-Aug. 2006 *ACI Structural Journal*, p. 551

Steel Fiber Concrete Slabs on Ground: A Structural Matter. Paper by Luca G. Sorelli, Alberto Meda, and Giovanni A. Plizzari

Discussion by Shiming Chen

Professor, School of Civil Engineering, Tongji University, Shanghai, China.

The authors attempted to develop a tentative design method in assessment of the load-carrying capacity of steel fiber-reinforced concrete (SFRC) ground slabs. The discusser appreciates the authors' comprehensive work carrying testing and FE parametric analysis on SFRC ground slabs. Some findings are interesting to the discusser, however, were not well clarified. Discussion is drawn as follows.

Experimental study

The tests demonstrated the significant enhancement of steel fiber to the bearing capacity and the ductility of concrete slabs on ground. Accordingly, it is indicated that the ultimate load was conventionally defined as corresponding to a sudden change of the monitored displacement that evidence the formation of a collapse mechanism full-developed crack surface along the medians or the diagonals. It looks likely that the maximum load levels illustrated in Fig. 4 and 5 of the paper are higher than the ultimate loads given in Table 6, and the SFRC ground slabs are capable of subjecting to further load even after the formation of a collapse mechanism. It is not clear what criterion is used in determining the ultimate load for each specimen. Is it judging by the sudden change of the monitored displacement or judging by the peak load level in the load-displacement curves?

To assess the effect of steel fiber on a ground slab, the load levels (where crack initiates in the ground slab) are very important, especially when the slab design is governed by crack control. Whereas it is not well clarified when the first crack initiated for each specimen, which was reinforced with different types of steel fibers and in different mixing dosages, are they inherent in a similar cracking load level, for example, 100 kN?

A comparison of the fracture properties given in Table 5 of the original paper demonstrates that there was a substantial increase in the fracture energy G_F and crack opening w_{ck} for SFRC specimens over the plain concrete specimen (S6), but the cracking stress levels (σ_{ct}) are almost the same. Figure A illustrates that the F/F_0 varies with the fracture energy G_F derived from Tables 5 and 6, where F is the collapse load of the ground slab and F_0 is the collapse load of the control specimen S_0. It appears that adding fibers in concrete enhances the collapse load of the ground slabs; however, the bearing capacity of the slabs decreases with the fracture energy for slabs with a single type of longer fiber (steel fiber 50/1.0), such as Slabs S4, S8, and S11, in a volume ratio of fiber 0.38 and 0.57%, respectively, but increases for Slabs S3 and S14, with hybrid longer and shorter fibers, in a volume ratio of 0.57%. It would be explained by the better efficiency of

shorter fibers and likely that mixed fiber reinforcement is more effective.

The final crack patterns of slabs demonstrated in Fig. 6 of the original paper are quite similar, characterized by cracks developed along the median lines and fewer along the diagonals. In terms of simple plastic analysis based on energy method, the load enabling different collapse mechanisms would be different. Can the authors explain why the numerical development of the crack patterns shown in Fig. 10 is different? For example, there are diagonal crack patterns in S0, S1, S4, S8, and S11, but median crack patterns in S3, S5, and S14. What governs these crack patterns?

Finite element model

There was uplift at the slab corners, as shown in Fig. 11 of the original paper, and this phenomenon was also observed and discussed in References 26 and 27. To evaluate realistic ultimate and service loads of a ground slab, it is necessary to take into account this nonlinearity between the foundation and the slab. In numerical modeling, the elastic soil was modeled by 616 linear elastic truss elements, which would be sharply different from the realistic situations as the uplifts developed at the slab corners, which would introduce substantial downward forces on the slab. The unilateral nonlinear elastic-plastic curve for the Winkle-type model proposed by Cerioni[26] would be better.

It is noted that the load-displacement curves based on the finite element analysis agree well with the test curves. However, would the load in numerical curves increase further or drop when the collapse mechanism developed, as defined in the original paper?

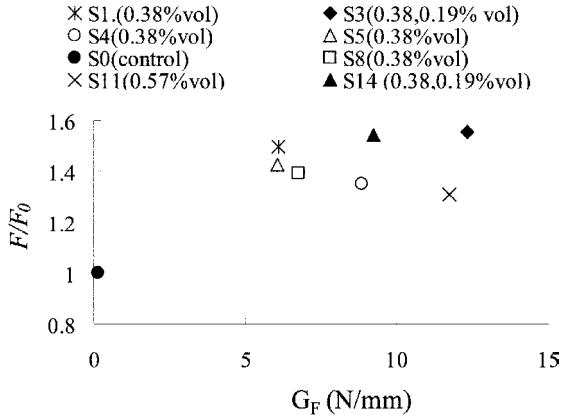

Fig. A—F/F_0 *varies with fracture energy* G_F.

Table A—Comparison of collapse loads

Slab no.	$F_{u,exp}$, kN	Steel fiber				$1 + R_{e,3}$
		50/1.0 %vol	30/0.6 %vol	20/0.4 %vol	12/0.18 %vol	
S0	177.0	—	—	—	—	1.0
S1	265.0	—	0.38	—	—	1.497
S3	274.9	0.38[(a)]	—	—	0.19	1.553
S4	238.6	0.38[(a)]	—	—	—	1.348
S5	252.3	—	0.38	—	—	1.425
S8	246.2	0.38[(b)]	—	—	—	1.391
S11	231.9	0.57[(a)]	—	—	—	1.310
S14	273.0	0.38[(b)]	—	0.19	—	1.542

Notes: F_0 is collapse load of control slab (S0); (a) and (b) refer to steel fiber type; 1 kN = 0.2248 kip.

Design method

Although there appears to be good correlation between the collapse loads of the approximated equation (Eq. (1) of the original paper) and the NLFM model, the contribution and physical interpretation of each parameter is not clear and it is difficult to apply it in design practice. A unit scale analysis of Eq. (1) leads to $[N]^{0.999}[mm]^{0.001}$. The seven coefficients (α_1, α_2, α_3, α_4, α_5, c_1, and c_2) should also be calibrated against test specimens whenever new fibers and different volume ratios are adopted.

The enhanced contribution of steel fiber on ground slabs is considered by introducing an equivalent flexural strength ratio or $R_{e,3}$ (at 3 mm [0.118 in.] deformation[28]). Let F_0 be the collapse load of a plain concrete ground slab; the collapse load of a SFRC ground slab is then expressed as

$$F_u = F_0 (1 + R_{e,3}) \quad (4)$$

where $R_{e,3}$ is the equivalent flexural strength ratio based on the flexural toughness test in accordance with JSCE-SF4.[29] For a typical hooked-end steel fiber (35/0.55, 0.38%vol), $R_{e,3}$ is 0.62, and a similar hooked-end steel fiber (60/0.92, 0.35%vol[30]) $R_{e,3}$ is 0.43.

Basically, the equivalent flexural strength ratio $R_{e,3}$ will depend on the aspect ratio of the fiber and the minimum overlapped spacing of the fiber within the concrete. No values of $R_{e,3}$ were reported for the tested slabs in the original paper, so one might guess that $R_{e,3}$ for tested slabs would be approximately 0.3 to 0.5. A comparison of the collapse loads of SFRC ground slabs against plain concrete ground slab derived from Table 6 of the original paper is given in Table A. The final column demonstrates the $1 + R_{e,3}$ derived from Eq. (1) based on the test results.

Additionally, the discusser has noticed the following possible miscalculations; could the authors please comment?

- k_w = 0.0785 kN/mm^3 (289.2 lb/in.^{3}) on page 555 and 0.21 kN/mm^3 (773.7 lb/in.^{3}) on page 556 should be k_w = 0.0785 N/mm^3 (289.2 lb/in.^{3}) and 0.21 N/mm^3 (773.7 lb/in.^{3}).

REFERENCES

26. Cerioni, R., and Mingardi, L., "Nonlinear Analysis of Reinforced Concrete Foundation Plates, *Computers and Structures*, V. 61, No. 1, 1996, pp. 87-106.

27. Chen, S, "Strength of Steel Fibre Reinforced Concrete Ground Slabs," *Structures and Buildings*, V. 157, No. SB2, 2004, pp. 157-163.

28. Concrete Society, "Concrete Industrial Ground Floors—A Guide to Their Design and Construction," *Technical Report* 34, Concrete Society, Slough, UK, 1994.

29. JSCE-SF4, "Method of Tests for Flexural Strength and Flexural Toughness of Steel Fibre Reinforced Concrete," *Concrete Library of JSCE*, 1984.

30. Roesler, J. R.; Lange, D. A.; Altoubat, S. A.; Rieder, K.-A.; Ulreich, G. R., "Fracture of Plain and Fiber-Reinforced Concrete Slabs under Monotonic Loading," *Journal of Materials in Civil Engineering*, ASCE, V. 16, No. 5, 2004, pp. 452-460.

AUTHORS' CLOSURE

The authors would like to thank the discusser for the interest and for the valuable discussion of the paper.

First of all, the authors would like to take this opportunity to underline an error in Tables 4 and 5 of the original paper, where S6 should be corrected in S0.

As far as the experiments are concerned, it should be observed that the load-carrying capacity of concrete slabs-on-ground is not exhausted even after the slab collapse

because the elastic springs under the bottom surface can carry further load. Indeed, the experimental failure of the SFRC slabs was neither sudden nor catastrophic because the elastic foundation keeps carrying further load. Other researchers[31,32] defined the failure load based on the formation of a crack pattern compatible with a yield line plastic mechanism. The identification of such crack patterns (throughout the bottom surface of the slab) during a slab test, however, is not an easy task. In all the experimental results, the authors observed a sudden variation of the displacement field (monitored by 16 LVDTs), which was conventionally defined as the slab collapse mechanism. Figure 9 of the original paper clearly shows the identification procedure.

The first crack load of the ground slabs was very difficult to measure because the first crack formed on the bottom surface of the slab. In the authors' opinion, however, the first crack load in fiber-reinforced concrete (FRC) slabs only depends on the tensile strength of the concrete matrix and not on the fiber type and content because fiber reinforcement starts activating after cracking of the concrete matrix and does not significantly contribute to prior cracking.

The fracture energy G_F is a significant parameter for material properties but may not be important in structures where the maximum crack opening at failure is very small (a few tenths of a millimeter), as in slabs-on-ground. In these structures, the fracture energy cannot fully develop in the cracked surfaces; however, FRC with shorter fibers develops more energy with smaller crack openings.[33]

As far as the numerical analyses are concerned, it should be noted that the collapse mechanisms can develop with cracks along the median or the diagonal lines. Previous numerical studies showed that the crack pattern depends on the slab stiffness related to the soils stiffness. In the slab specimens, these values are close to the border line so that cracks can develop either along the medial or the diagonal line.

Concerning the finite element model (FEM), it should be observed that all the numerical simulations of the slabs-on-ground stopped (no longer converged) at the slab collapse.

Furthermore, Belletti et al.[34] analyzed the experimental results by means of a multiple-crack model, which can be seen as an extension of the one proposed by Cerioni and Mingardi,[26] and accounted for the effect of the unilateral springs; their numerical results showed that the uplift at the slab corners has a minor influence on the ultimate load experimentally determined on the ground slabs.

As far as the design method is concerned, the authors would like to underline that the left term of Eq. (1) in the original paper is a force with the following fundamental physics dimensions: $[\text{Length}]^1\ [\text{Mass}]^1\ [\text{Time}]^{-2}$. The units calculated by the discusser as $[\text{N}]^{0.999}[\text{mm}]^{0.001}$ are likely due to the round-off error of the numerical solutions and should be reasonably approximated to the close integers (that is, 0.9999 ~ 1 and 0.001 ~ 0). The five coefficients (α_1, α_2, α_3, α_4, and α_5) are the powers law exponents of quantities (A_L, B, L, k_w, f_{res}, and f_{If}), which do have a clear physical significance, as explained in the original paper. Moreover, Eq. (1) fits more than 1000 numerical simulations (based on nonlinear fracture mechanics) with remarkable accuracy. The fitting equation can be considered valid within a wide range of applications (fiber type and content, matrix strength, and slab geometry), as considered in the original paper.

The authors appreciate the comparison with the flexural strength ratio $R_{e,3}$; however, because the crack opening at collapse in real slabs is very small, according to authors' opinion, parameters associated with a smaller crack opening could be more representative of the slab-on-ground behavior.

REFERENCES

31. Meyerhof, G. G., "Load Carrying Capacity of Concrete Pavements," *Journal of the Soil Mechanics and Foundation Division*, V. 88, No. 3, 1962, pp. 89-115.

32. Ottosen, N. S., "A Failure Criterion for Concrete," *Journal of the Engineering Mechanics Division*, V. 103, No. EM4, 1977, pp. 527-535.

33. Sorelli, L.; Meda, A.; and Plizzari, G. A., "Bending and Uniaxial Tensile Tests on Concrete Reinforced with Hybrid Steel Fibers," *Journal of Materials in Engineering*, ASCE, V. 15, No. 5, 2005, pp. 519-527.

34. Belletti, B.; Cerioni, R.; and Plizzari, G. A.,"Fracture in SFRC Slabs on Grade," *Proceedings of the 6th RILEM Symposium on Fibre Reinforced Concretes (FRC)*, M. di Prisco, R. Felicetti, and G. A. Plizzari, eds., RILEM PRO 39, Varenna, Italy, Sept. 2004, pp. 723-732.

Disc. 103-S61/From the July-Aug. 2006 *ACI Structural Journal*, p. 577

Strength of Struts in Deep Concrete Members Designed Using Strut-and-Tie Method. Paper by Carlos G. Quintero-Febres, Gustavo Parra-Montesinos, and James K. Wight

Discussion by Pedro R. Muñoz

PhD, PE, Principal, PRM Engineering, Structural Consulting Engineers, Newburyport, Ma.

The behavior of deep concrete members differs greatly from that of shallow concrete members. It appears that the load path for a point load applied at the top of a deep beam will follow a rather straight path from the point of application of the point load down to the points of support, which appears to deviate somewhat from that of a typical bending behavior for a point load applied at the top of a shallow concrete member.

That portion of the deep beam following the straight path of the axial compressive forces will behave very much like a strut in which case the strut-and-tie method of the ACI Building Code could be applied to evaluate the strength of the strut in the deep beam.

The authors of this paper have considered the main design variables for the experimental investigation of the strength of struts in deep concrete members: the angle between primary strut-and-tie axis, the amount of reinforcement crossing the strut, and the concrete strength, but failed to include any reinforcement in the section of the strut that will definitely have a significant increase effect in the total strength of the struts. The behavior of reinforced concrete columns has been investigated extensively, and it appears to be well understood for short and slender members under axial compressive forces and reinforced with longitudinal and transversal reinforcement. As part of the strength factors for struts in the strut-and-tie methods of the ACI Building Code, provisions shall be made to incorporate the contribution of steel reinforcement in the section of the strut that may become a reinforced strut. It is important to consider that not very well confined concrete

members under axial compressive forces will crack and fail in shear rather prematurely for axial loads exceeding the capacity and strength of the unreinforced concrete member; therefore, the contribution of steel reinforcement in the strut section becomes significant and provides an added axial strength component to the total strength of a reinforced strut in a strut-and-tie model similar to the contribution of steel and concrete in a reinforced concrete short column.

Similar to what is done with concrete columns that are reinforced vertically with steel bars, the same could be done with this strut portion of the deep concrete member, providing a much more higher axial load capacity, becoming this portion of a reinforced strut where both the concrete section of the strut and the steel bar embedded in the middle of the strut both contribute to the axial load in proportion to their corresponding cross-sectional properties of concrete and steel.

The aforementioned concept can be described in the revised Fig. 2 from the paper (Fig. A herein), by adding a steel reinforcement bar or bars in the section of the strut that will resist part of the concentrated Load P. This bar is labeled as A_{st} inside the strut section. Practically speaking, this should not be difficult to achieve in the field and it should not be any more difficult to install than any of the transverse or longitudinal reinforcement in the concrete member. It would be interesting to see if the authors of this paper could undertake another series of tests by adding the suggested steel reinforcement in the section of the struts and compare the ultimate achieved loads for the specimens with the modified reinforced struts. If possible, other steel reinforcement bars could also be added to the other strut sections of the entire strut-and-tie model of the deep concrete member. This could be a new trend to achieve higher loads in concrete members behaving in a manner consistent with the strut-and-tie model.

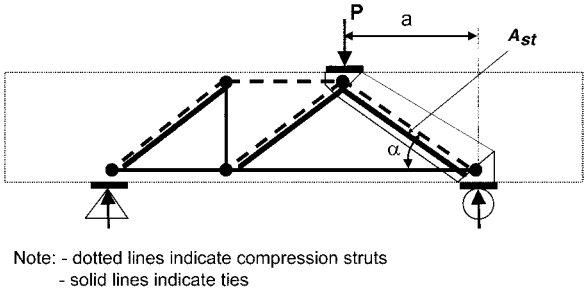

Fig. A—Strut-and-tie model for deep beam design.

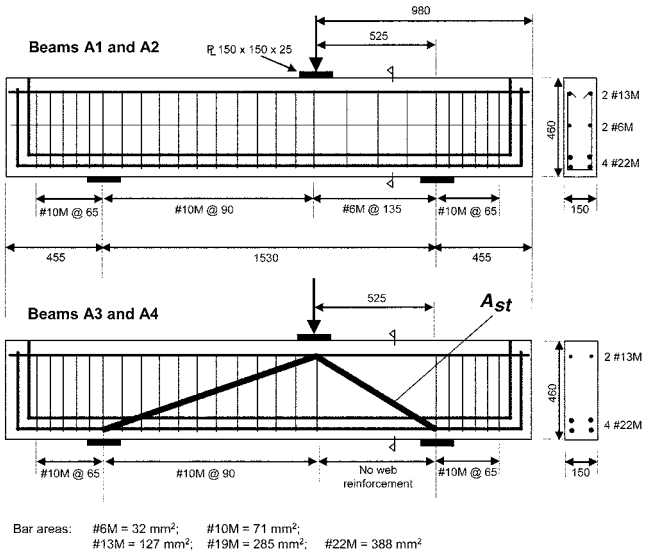

Fig. B—Reinforcement details for Series A.

The revised Fig. 3 from the paper (Fig. B herein) indicates the suggested additional steel reinforcement labeled A_{st} in the sections of the struts. Equation (1) of the paper presents the strength of a concrete strut expressed as a function of the concrete compressive strength; again herein, it is suggested to add the contribution of the steel reinforcement to the strength of the strut and modify the equation to include the contribution of both steel and concrete. Other efficiency factors could be evaluated and incorporated into the final equation after a calibration of the tests and analytical studies are correlated.

The investigators of this paper have considered two amounts of reinforcement crossing the primary strut, It appears that a more effective contribution of steel reinforcement to the behavior and strength of the strut in deep concrete members could be achieved by incorporating a longitudinal steel reinforcement embedded right into the strut section—it will definitely prove to be more effective than the reinforcement crossing the strut.

Instead of very complicated expressions for the contribution of concrete in the strength of the strut, it would be more beneficial to incorporate the steel reinforcement and come up with expressions for the combined strength of the reinforced strut similar to what is currently done for reinforced concrete columns, with the appropriate modification and possibly efficiency factors suited for the case of deep concrete members. Therefore, Eq. (2) through (4) would have another term that would include the contribution of the steel reinforcement to the total strength of the reinforced strut.

It would be interesting to see how the load-displacement curves shown in Fig. 6 and 7 would look like after the specimens with the modified reinforced struts similar to what is shown in the revised Fig. 3 (Fig. B herein) are tested and the loads and deflections plotted for comparisons.

The cracking patterns most likely will change and the strains in the longitudinal and transverse reinforcement will be most likely lower than those in the specimens tested in this paper.

The authors have noted in the section Strains in web or strut reinforcement that, "the strain measurements and visual observations indicated that the web reinforcement was effective in controlling crack opening." Having steel reinforcement in the strut sections will most likely reduce the cracking due to diagonal stresses along the path of the load through the strut to the support because the concrete alone will not carry all the combined stresses in the strut.

As the authors of this paper mention in one of the paragraphs before the Summary and Conclusions section, "Clearly additional experimental information needs to be generated to draw definite conclusions with regard to the minimum web reinforcement required in high-strength concrete members designed using strut-and-tie models." It appears that perhaps the additional experimental information that could be undertaken in future research on this subject could be oriented toward having some type of reinforcement in the strut sections, which will clearly provide additional strength to the strut-and-tie models.

This comment addresses Item 2 of the Summary and Conclusions, where clearly the transverse reinforcement alone without any kind of steel reinforcement in the strut section will not provide a reliable strength capacity of the strut section.

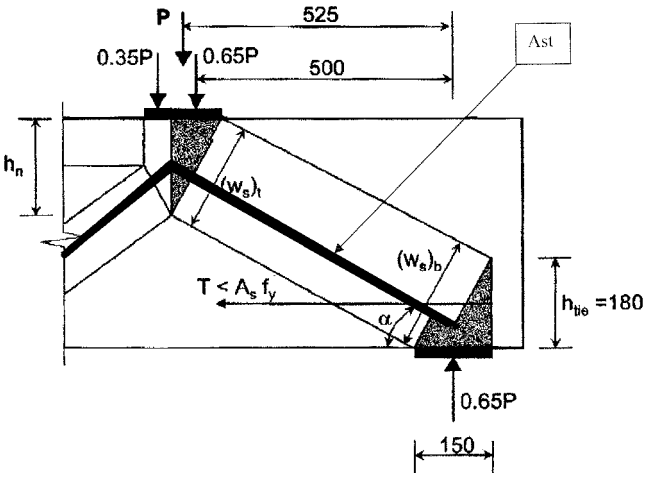

Fig. C—Strut-and-tie model in critical span of Specimen A1.

The revised Fig. A-1 (Fig. C herein) indicates the strut-and-tie model in the critical span section of the specimen tested and analyzed, with a steel reinforcement labeled A_{st} in the middle of the strut section. Clearly, this could be treated as a short column, and, as such, the total strength provided by the combination of both the concrete in the strut and the added reinforcement will be much higher than what is calculated with the expressions and equation shown in the Appendix.

The diagonal steel reinforcement in the strut A_{st} becomes a principal diagonal reinforcement of the deep concrete beam. This is not a current practice, but it is very effective and an inexpensive way to reinforce the diagonal strut in the deep concrete members and to enhance the load-carrying capacity of the deep concrete member.

It would be interesting to know what the authors think about the possibility of extending their research work by incorporating a reinforced strut section and studying the failure modes to see what enhancements could be achieved by reinforcing the compressive strut in the deep concrete beams.

A suggestion to the authors and future researches will be to look into incorporating some type of steel reinforcement in the strut section as shown in Fig. A; A_{st} will be the steel bar in the concrete strut, making it a reinforced concrete strut.

AUTHORS' CLOSURE

The authors would like to thank the discusser for his interest in the paper. The use of steel reinforcement in the longitudinal direction of the concrete diagonal struts was not investigated because the authors do not believe it represents typical practice for the design of deep concrete members. The discusser should notice, however, that the use of such reinforcement to increase the strength of concrete struts is discussed in Section A.3.5 of the 2005 ACI Building Code.

Disc. 103-S64/From the July-Aug. 2006 *ACI Structural Journal*, p. 604

Experimental Investigations on Punching Behavior of Reinforced Concrete Footings. Paper by Josef Hegger, Alaa G. Sherif, and Marcus Ricker

Discussion by Himat T. Solanki

ACI member, Professional Engineer, Building Department, Sarasota County Government, Sarasota, Fla.

The authors have presented an interesting paper on punching behavior of reinforced concrete footings. However, the discusser would like to offer the following comments:

1. The discusser has reviewed several publications[12-22] regarding the punching shear failure cone angle. Based on the literature, the punching cone angle depends on the thickness of footing slabs, the amount and arrangement of reinforcement, strength of concrete, and the ground stiffness (Fig. A). The discusser believes that the range of cone angle should be between 25 to 60 degrees. Therefore, the authors conclusion No. 1 may be based on their limited data and cannot be generalized.

2. Though the ground stiffness has some influence[12,13,18,21,22] on the punching shear strength but it may be neglected.

3. The discusser believes a similar paper has been published in the German magazine *Beton und Stahlbetonbau*, V. 101, No.4, 2006, by the senior author and his colleagues.

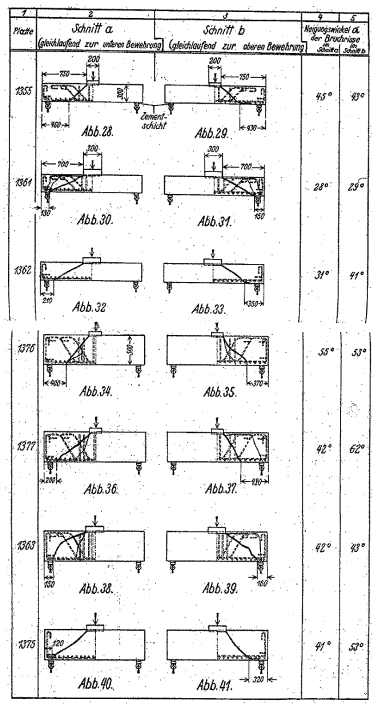

Fig. A—Crack angles with respect to slab thickness, reinforcement, and concrete strength.[14]

REFERENCES

12. Talbot, A. N., "Reinforced Concrete Wall Footings and Columns Footings," *Bulletin* 67, University of Illinois Experiment Station, University of Illinois, Urbana, Ill., Mar. 1913.

13. Moe, J., "Shearing Strength of Reinforced Concrete Slabs and Footings under Concentrated Loads," *Research and Development Bulletin* D47, Portland Cement Association, Skokie, Ill., Apr. 1961.

14. Graf, O., "Versuche über die winderstandsfähigkeit von allseitig Aufliegenden Dicken Eisenbetonplatten unter Einzellasten," No. 88, Deutscher Ausschuss für Eisenbeton, Berlin, Germany, 1938.

15. Dieterle, H., "Zur Bemessug von Fundamentplatten ohne Schubbewehrung," *Beton und Stahlbetonbau*, V. 73, 1978, pp. 20-37.
16. Aster, H., and Koch, R., "Schubtragfähigkeit dicker Stahbetonplatten," *Beton und Stahlbetonbau*, No. 11, 1974, pp. 266-270.
17. Hillerborg, A., "Förankringssäkerhet hos konstruktioner utan skjuvarmering," *Nordisk Betong*, No. 2, 1959, pp. 119-138.
18. Hallgren, M.; Kinnunenm, S.; and Nylander, B., "Punching Shear Tests on Column Footings," *Technical Report* 1998:3, Department of Structural Engineering, Royal Institute of Technology, 1998.
19. Matthaei, O., and Tue, N. V., "Punching Shear Behaviour of Foundation Slabs," *Proceedings of the International Workshop on Punching Shear Capacity of RC Slab*, Stockholm, Sweden, 2000, pp. 83-90.
20. Sonobe, Y. et al., "Experimental Study on Size Effect in Pull-Out Shear Using Full Size Footings," *Size Effect in Concrete Structures*, H. Mihashi, H. Okumura, and Z. P. Bažant, eds., E&FN Spon., London, 1994, pp. 105-116.
21. Lebelle, P., "Semelles de Béton Armé," *International Association for Bridge and Structural Engineering*, V. 4, 1936, pp. 379-409.
22. Silfwerbrand, J., "Punching Shear Capacity of Steel Fibre Reinforced Concrete Slabs on Grade," *Proceedings of the International Workshop on Punching Shear Capacity of RC Slab*, Stockholm, Sweden, 2000, pp. 485-493.

Disc. 103-S65/From the July-Aug. 2006 *ACI Structural Journal*, p. 614

Simplified Modified Compression Field Theory for Calculating Shear Strength of Reinforced Concrete Elements.

Paper by Evan C. Bentz, Frank J. Vecchio, and Michael P. Collins

Discussion by Himat T. Solanki

ACI member, Professional Engineer, Building Department, Sarasota County Government, Sarasota, Fla.

1. The authors have presented an interesting paper. The discusser is somewhat confused about the intent of the paper. This paper does not provide any design-oriented or codified design concept. This paper is merely a theoretical approach of previously published papers by the senior authors on this subject, that is, modified compression field theory (MCFT). Normally, the modified version improves the mean and coefficient of variation (COV) values, but this paper presents a higher number of scatter results (–0.09 to +0.48) than the previously published papers. In the paper, all specimens have higher $v_{exp}/v_{predicted}$ values except Panels PV2, TP5, PP3, and VA4 in comparing the MCFT with the simplified MCFT, but no explanation was given by the authors. Also in this paper, the authors have primarily analyzed the University of Toronto and the University of Houston panels and approximately 50% Obayashi Corp., Japan, panels. The discusser has plotted a set of curves, as shown in Fig. A, and compares them with other curves. Based on Fig. A, it can be seen that the authors' curve falls quite far below all of the other curves; therefore, the authors' proposed method predicts scatter results.

2. The authors stated that "The MCFT β values for elements without transverse reinforcement depend on both ε_x and s_{xe}." The discusser believes that the crack width is much more important[42,43] than the s_{xe} values.

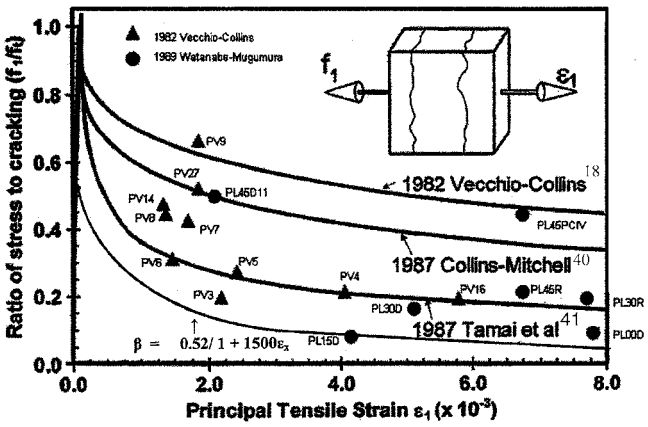

Fig. A—Ratio or stress to cracking (f_1/f_t) versus principal tensile strain ε_1 (ε_x) ($\times 10^{-3}$).[39]

3. The authors have developed Eq. (28) from the reinforcement in only the *z*-direction and 12 in. (304.8 mm) crack spacing, which is contrary to the published data. Also, if one can assume $\varepsilon_x = 0$ and $s_{xe} = 0$, an angle θ would become approximately 25.5 degrees, which is also contrary to Joint ACI-ASCE Committee 445.[44] Therefore, Eq. (28) has very limited applicability. Joint ACI-ASCE Committee 445[44] mentioned that the angle θ can be computed when the shear stresses are less than those causing first yield of a reinforcement

$$\tan^4\theta = (1+(1/n\rho_x))/(1+(1/n\rho_y)) \quad (33)$$

Hsu[45] proposed the following equation by assuming yielding of steel

$$\cot\theta = \sqrt{\rho_x f_{sxy} / \rho_z f_{szy}} \quad (34)$$

4. The discusser has reviewed and analyzed the University of Toronto reinforced panels, which the authors have not included in their analysis, having unsymmetrical reinforcement[36] and reinforced concrete panels with perforations[37] using the simplified MCFT and a similar performance, that is, scatter results, as outlined in the paper, was found. Is a proposed theory applicable to these types of structures? In practice, this type of condition always exists.

5. The discusser has analyzed the numerous panels using a very simple practical approach as outlined in the following. To calculate the shear stress τ_{xz}, Sato and Fujii's[46] equations were simplified and rearranged as follows

$$\tau_{xz} = \sigma_{c1m}\tan\theta_m + \sigma_x f_{sxy}\tan\theta_m \quad (35)$$

$$\tau_{xz} = \sigma_{c1cr}\tan\theta_{cr} + \sigma_x f_{sxy}\tan\theta_{cr} \quad (36)$$

$$\tau_{xz} = \sigma_{cn}\tan\varphi - \tau_{ct} + \sigma_x f_{sxy}\tan\varphi \quad (37)$$

To calculate σ_{c1m} and σ_{c1cr}, Kupfer[47] suggested the following equation for concrete subjected to biaxial tension-compression stresses

$$\sigma_{c1m} \text{ or } \sigma_{c1cr} = f_t(1 - 0.7(\sigma_{c2}/f'_c)) \quad (38)$$

To calculate the value σ_{c2}/f'_c, Schlaich et al.[48] have suggested several values for different effective stress levels in concrete struts and have outlined them in Table 1 of Reference 44. Therefore, $\sigma_{c2}/f'_c = Kf'_c$ could be taken.

The value K equals the effective stress level constant and f_t can be taken as Joint ACI-ASCE Committee 445.[45]

$$f_t = 0.33\sqrt{f_c'}/(1 + \sqrt{500\varepsilon_1}) \quad (39)$$

where $\varepsilon_1 = \varepsilon_x + (\varepsilon_x + \varepsilon_2)\cot^2\theta$; ε_x equals the strain in the tension tie = 0.002; ε_2 equals the strain in the compression strut = 0.002; θ equals the angle between the strut and the tension tie.

To calculate τ_{ct} and σ_{cn}, Walraven[49] suggested the following formulas for shear stress τ_{ct} and compressive stress σ_{cn}

$$\tau_{ct} = (-f_{cube}/3) + [1.8\delta_n^{-0.8} - (0.234\delta_n^{-0.707} - 0.2)f_{cube}]\delta_t \quad (40)$$

$$\text{when } \tau_{ct} > 0$$

$$\sigma_{cn} = (-f_{cube}/20) + \left[1.35\delta_n^{-0.63} - \left(0.191\delta_n^{-0.552} - 0.15\right)f_{cube}\right]\delta_t \quad (41)$$

$$\text{when } \sigma_{cn} > 0$$

where $f_{cube} = 1.1f'_c$, δ_t equals the slip across crack, and δ_n equals the normal displacement across crack.

The crack width can be expressed as

$$w_{cr} = \sqrt{\delta_t^2 + \delta_n^2} \quad (42)$$

Also, concrete stresses at the crack can be related to[47]

$$\sigma_{c1cr} = \tau_{ct}\tan\theta + \sigma_{cn} \quad (43)$$

Assuming crack width as suggested by Beeby[42] and Walraven and Reinhardt[41] and considering Eq. (33) through (43), the discusser has analyzed 297 panels (including the authors 102 panels) and found them to be in very good agreement with the test values ($v_{exp}/v_{predicted}$ = 1.011 and COV 5.91%) as compared with the authors' scatter results from their simplified MCFT.

The discusser believes that the simplified concept could also be used for calculating the shear strength of reinforced concrete elements based on the crack width and can be applied to any code that recommends/limits the crack width as compared with the authors proposed theory/simplified MCFT.

ACKNOWLEDGMENTS

The discusser gratefully acknowledges S. Unjoh, Leader, Earthquake Engineering Team, Public Works Research Institute, for providing Japanese publications related to the shear panels.

REFERENCES

39. Bentz, E. C., "Explanation the Riddle of Tension Stiffening Models for Shear Panel Experiments," *Journal of Structural Engineering*, ASCE, V. 131, No. 9, Sept. 2005, pp. 1422-1425.

40. Collins, M. P., and Mitchell, D., *Prestressed Concrete Basics*, Canadian Prestressed Concrete Institute, Ottawa, Canada, 1987.

41. Tamai, S. et al., "Average Stress-Strain Relationship in Post Yield Bar in Concrete," *International Concrete Library,* JSCE, No. 11, 1987, pp. 117-129.

42. Beeby, A. W., "Cracking: What are Crack Width Limits For?" *Concrete*, July 1978, pp. 31-33.

43. Walraven, J. C., and Reinhardt, H. W., "Theory and Experiments on the Mechanical Behaviour of Cracks in Plain and Reinforced Concrete Subjected to Shear Loading," *Heron*, V. 26, No. 1A, 1981, 68 pp.

44. Joint ACI-ASCE Committee 445, "Recent Approach to Shear Design of Structural Concrete," *Journal of Structural Engineering*, ASCE, V. 124, No. 12, Dec. 1998, pp. 1375-1417.

45. Hsu, T. T. C., "Stress and Crack Angles in Concrete Membrane Elements," *Journal of Structural Engineering*, ASCE, V. 124, No. 12, Dec. 1998, pp. 1476-1484.

46. Sato, Y., and Fujii, S., "Local Stresses and Crack Displacements in Reinforced Concrete Elements," *Journal of Structural Engineering*, ASCE, V. 128, Oct. 2002, pp. 1263-1271.

47. Kupfer, H., "Das Verhalten des Betons unter mehrachsiger Kurzzeitbelasting," Deutscher Ausschuss fur Stahlbetopn, No. 229, 1973.

48. Schlaich, J.; Schafer, I.; and Jennewein, M., "Towards a Consistent Design of Structural Concrete," *Journal of Prestressed Concrete Institute*, V. 32, No. 3, 1987, pp. 74-150.

49. Walraven, J. C., "Fundamental Analysis of Aggregate Interlock," *Journal of Structural Engineering*, ASCE, V. 107, No. 11, Nov. 1981, pp. 2245-2270.

AUTHORS' CLOSURE

The discusser is thanked for his interest in the paper on the MCFT. The issues raised will be commented on in the order presented by the discusser.

1. The discusser seems to have missed the intent of the paper. As noted in the abstract, "this paper presents a new simplified analysis method that can predict the strength of…panels in a method suitable for 'back of the envelope' calculations." Thus, the authors were not trying to produce a method with improved statistical properties, but rather one that was easier to use. The MCFT requires that 15 nonlinear equations be solved simultaneously for any given load level. With the newly presented simplified MCFT, which has been implemented into the Canadian concrete code,[4] only four equations are required.

Figure A is derived from a paper by the first author and shows principal tensile stress on the vertical axis.[39] The discusser appears to have plotted shear stresses on this same axis, which results in an inappropriate comparison. As shown in Table 1 of the paper, the scatter associated with the full MCFT can be expressed as a coefficient of variation (COV) of 12.2%, whereas the simplified MCFT has a COV of 13.0%. Thus, the authors disagree that the new method produces significantly more scattered results than the more complex "full" MCFT.

2. The authors agree that crack width is the crucial concept in determining the parameter β. Crack widths can be estimated by multiplying the average spacing of the cracks by the average strain perpendicular to the cracks. In the simplified MCFT, the parameter s_{xe} represents the crack spacing and ε_x represents the strain. While these two parameters are determined in the x-axis direction rather than the diagonal direction, the concept is the same: the β equation is based on an estimate of crack width.

3. Equation (28), which presents the angle θ for calculation of transverse reinforcement effectiveness and demand on longitudinal reinforcement, was derived based on the MCFT equations. The derivation of this equation was not presented in this paper as it is available in another paper published elsewhere.[50] The authors disagree that Eq. (28) is of limited applicability and simply note that in the preparation of Table 1, no significant residual trends were observed with respect to the different input variables as would be expected if it were

of limited applicability. Equation (33), as presented by the discusser, is not appropriate for methods like the simplified MCFT that assume the transverse reinforcement has yielded at shear failure. Equation (34) is based on plasticity and assumes that both directions of steel are yielding at failure. As shown in Fig. 9, specimens that fail in this way are modeled well by the simplified MCFT.

4. As noted in the paper, the simplified MCFT is directed toward members subjected to shear combined with uniaxial tension or compression as in a beam or column. All six elements loaded this way in Reference 36 were included in the paper. Reference 37 examined the effects of having a large opening in the shear panel and elements with such a hole were not included in the paper as the hole would produce a disturbed stress field. Of the two repeat experiments without openings in Reference 37 that were not biaxially loaded, the one with the lower strength was included in Table 1. Arguably, element PC1A should have been included instead of PC1 as PC1 suffered a premature edge failure,[37] but the lower strength was used in Table 1. No elements available to the authors that met the restrictions on loading were ignored or discounted in the preparation of the paper. It appears that the discusser has found additional tests from Japan and the authors look forward to testing the method against these results as well.

5. The analysis method presented in Item 5 appears to be a combination of strut-and-tie equations with equations from multiple other sources. Without the results of these calculations presented, or even the number of tests used in the discusser's statistical analysis, it is difficult to comment on the method as presented. The authors look forward to being able to examine it in more detail when it is published. It is clear, however, that the method proposed by the discusser requires the solution of at least 11 nonlinear equations, and thus is, again, aimed at a different user than the simplified MCFT.

REFERENCES

50. Bentz, E. C., and Collins, M. P., "Development of the 2004 CSA A23.3 Shear Provisions for Reinforced Concrete," *Canadian Journal of Civil Engineering*, V. 33, No. 5, May 2006, pp. 521-534.